Marine Geology 385 (2017) 185–203

Contents lists available at ScienceDirect

Marine Geology

journal homepage: www.elsevier.com/locate/margo

Cenozoic North Atlantic deep circulation history recorded in contourite drifts, offshore Newfoundland, Canada

Patrick R. Boyle [a,*,1], Brian W. Romans [a], Brian E. Tucholke [b], Richard D. Norris [c], Stephen A. Swift [b], Philip F. Sexton [d]

[a] Department of Geosciences, Virginia Polytechnic Institute and State University, Blacksburg, VA 24061, USA
[b] Department of Geology and Geophysics, Woods Hole Oceanographic Institution, Woods Hole, MA 02543, USA
[c] Scripps Institution of Oceanography, University of California San Diego, La Jolla, CA 92093-0244, USA
[d] School of Environment, Earth & Ecosystem Sciences, The Open University, Milton Keynes MK7 6AA, UK

ARTICLE INFO

Article history:
Received 27 August 2016
Accepted 26 December 2016
Available online 19 January 2017

Keywords:
Seismic stratigraphy
Contourite drifts
Abyssal circulation
J-Anomaly Ridge
Southeast Newfoundland Ridge
North Atlantic Ocean

ABSTRACT

In the North Atlantic Ocean, contour-following deep currents have created regional erosional unconformities and deposited contourite drifts that exceed 2 km in thickness and extend for 100 s of km. The stratigraphic records in the drifts have been used to reconstruct variations in North Atlantic deep-water circulation throughout the Cenozoic; however, uncertainties remain about certain aspects of the timing, intensity, depth distribution, and regional impact of these currents. Here, we use an integrated dataset of seismic-reflection profiles and IODP core data (lithology, biostratigraphy, and magnetostratigraphy) to document sedimentation history and the development of current effects in the Cretaceous to present sedimentary record on the J-Anomaly Ridge and Southeast Newfoundland Ridge, offshore Newfoundland, Canada. The Newfoundland ridges are in a key location, lying between well-studied areas in the northern and western North Atlantic and under the path of both the modern Deep Western Boundary Current and the Gulf Stream. Late Cretaceous through Early Eocene sedimentation on the ridges was dominated by biogenic pelagic sedimentation, but at ~47 Ma, near the Early-Middle Eocene boundary, well developed contourite drifts began to accrete in paleo-water depths of ~4000–4500 m, accompanied by an order-of-magnitude increase in terrigenous sediment mass accumulation rates. From this time forward, drift deposition, interrupted by brief episodes of erosion, continued unabated. This timing for the onset of persistent deep currents is coincident with reorganization of Atlantic circulation inferred from a change from biosiliceous to non-biosiliceous sedimentation in the western North Atlantic (Horizon A^C) and with the current-eroded Intra-Eocene Unconformity (IEU) in the northern North Atlantic. A change in sedimentation style occurred within the Middle Eocene to upper Oligocene drift sequence, and it likely was related to a shift to deeper, more intense currents that eroded the widespread Horizon A^U along the margin of eastern North America about Early Oligocene time. Beginning in the Late Oligocene (~25 Ma) a thick drift exhibiting seismically laminated mudwaves was deposited in a distinct belt at ~3500–4500 m paleodepth on the Southeast Newfoundland Ridge. This development correlates with widespread Late Oligocene through Miocene-Pliocene drift accumulation throughout the North Atlantic. The most recent phase of drift deposition, since Late Pliocene time (~3 Ma), occurred after a shift to the 'modern' circulation system of deeper, swifter currents, and it includes mixed pelagic-hemipelagic sediments and ice-rafted debris that reflect glacial-interglacial influences on sedimentation.

1. Introduction

In the North Atlantic Ocean, southerly flowing, contour-following deep currents have been associated with development of regional unconformities and deposition of contourite drift deposits that exceed 2 km in thickness and extend for 100's of km (Heezen and Hollister, 1964; Heezen et al., 1966; Tucholke and Mountain, 1979; Mountain and Tucholke, 1985; Faugères et al., 1999; Stow et al., 2002; Rebesco et al., 2014). In the modern ocean, the southerly flow of the Deep Western Boundary Current and underlying southward-flowing Antarctic Bottom Water (AABW) comprise the primary deep current system along the continental margin of the western North Atlantic Ocean basin (Fig. 1) (McCave and Tucholke, 1986; Bower and Hunt, 2000; Stow et al., 2002; Rahmstorf, 2006). The stratigraphic records in contourite drifts that formed along the path of the progenitor of this

* Corresponding author.
E-mail address: prboyle@vt.edu (P.R. Boyle).
[1] Present Address: ConocoPhillips Company, Houston, TX, 77079 USA.

http://dx.doi.org/10.1016/j.margeo.2016.12.014
0025-3227/

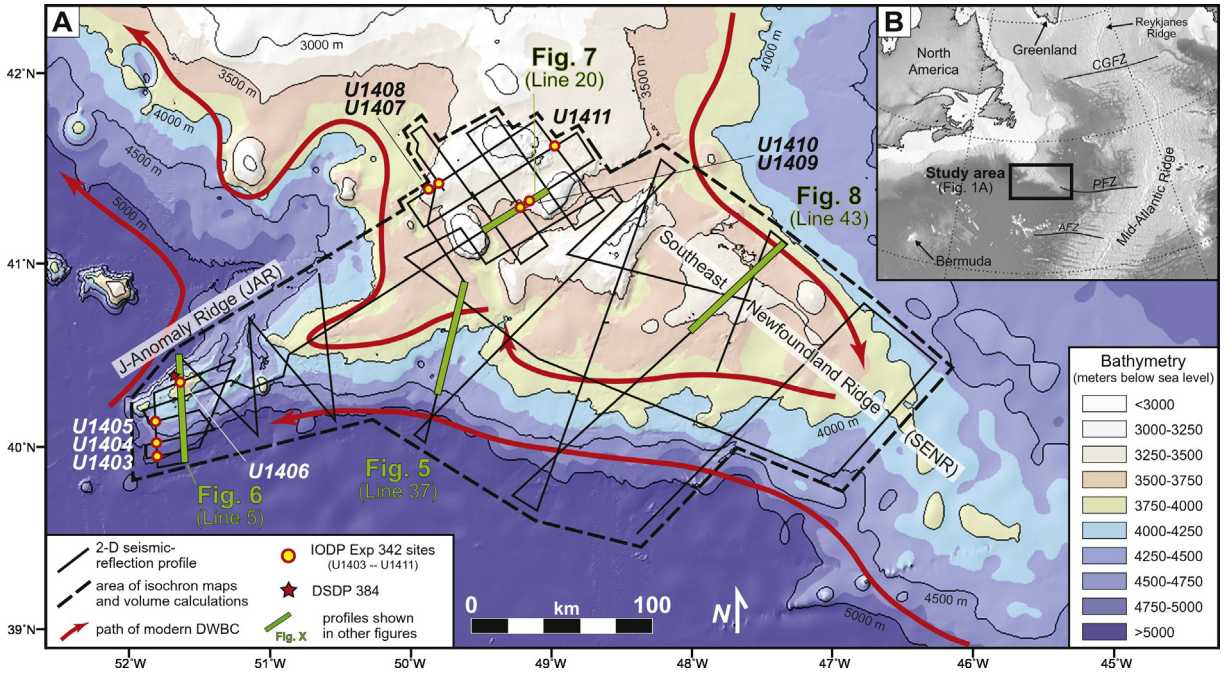

Fig. 1. (a) Bathymetric map of the J-Anomaly Ridge (JAR) and Southeast Newfoundland Ridge (SENR), offshore Newfoundland, Canada. Solid black lines show seismic-reflection profiles acquired during R/V Knorr Cruise 179-1 (Norris et al., 2004). The dashed polygon shows the limits of the area mapped. Thick red lines show the path of the modern Deep Western Boundary Current (DWBC), which consists of Labrador Sea Water in its upper part, Norwegian-Greenland Sea Overflow water at intermediate depths, and Antarctic Bottom Water below ~4500 m on the south side of the Newfoundland ridges (McCave and Tucholke, 1986). IODP Exp 342 drill sites are shown as red points with yellow centers and DSDP Site 384 is a black and red star. Thick green lines show locations of seismic profiles in Figs. 5–8. (b) Map of the North Atlantic Ocean showing regional bathymetric features and location of box in part A. CGFZ = Charles Gibbs Fracture Zone; PFZ = Pico Fracture Zone; AFZ = Atlantis Fracture Zone). Bathymetric base map for (a) and (b) is from GeoMapApp (http://www.geomapapp.org). (For interpretation of the references to color in this figure legend, the reader is referred to the web version of this article.)

deep current system have been used to infer variations in deep-water circulation throughout the Cenozoic (e.g., Berggren and Hollister, 1974; Tucholke and Ewing, 1974; Tucholke and Mountain, 1979; Mountain and Tucholke, 1985; Davies et al., 2001; Hohbein et al., 2012). For simplicity, we hereafter refer to the southerly flow of bottom water along the continental margin as the DWBC, irrespective of its specific sources, density, and depth range during the Cenozoic.

The Cenozoic is a period that experienced "Greenhouse" warming and long-term (10^7 yr) global cooling as well as several short-term ($<10^6$ yr) global-scale climate shifts/events (Zachos et al., 2001, 2008) that affected deep circulation. While the local to regional effects of many of these circulation events are relatively well known, there are still significant uncertainties about: 1) the times at which abyssal circulation was stimulated by sinking of cold, dense surface water at various high-latitude locations, 2) depths at which the resulting deep currents flowed, 3) regional vs. local geologic significance of the flows, and 4) correlation of circulation events throughout the North Atlantic ocean basins. For example, proposed dates for the onset of significant deep-water formation in the high-latitude North Atlantic vary from as old as Early Eocene to as young as Early Miocene (Miller and Tucholke, 1983; Davies et al., 2001; Hohbein et al., 2012; Müller-Michaelis et al., 2013). It has also been proposed that southern-sourced bottom water was responsible for erosion on the southwestern Bermuda Rise as early as Late Paleocene time (Mountain and Miller, 1992), and southern-sourced bottom water may have contributed significantly to later circulation events (Norris et al., 2001).

The Newfoundland ridges, southeast of the southern Grand Banks (offshore Newfoundland, Canada), include the J-Anomaly Ridge (JAR) and Southeast Newfoundland Ridge (SENR) (Fig. 1). The JAR and SENR are ideally located to record the activity of the DWBC because the current is constrained by the overturning circulation in the North Atlantic to flow around the ridges. This area is also influenced by the Gulf Stream and its northward extension as the North Atlantic Current, which have been shown to extend to the seafloor both north and south of the SENR (e.g., Savidge and Bane, 1999; Meinen and Watts, 2000). In addition, the deep (~>4500 m) southern margins of the JAR and SENR are presently affected by the southern-sourced AABW (Richardson et al., 1981; McCave and Tucholke, 1986; Norris et al., 2001).

The JAR and SENR are mantled with sediments that have accumulated since the Early Cretaceous, and current-controlled sedimentary drifts there are well developed in the Cenozoic section. The area is well suited to examine contourite development because it is topographically isolated from downslope sediment transport from the adjacent Grand Banks. The entire sedimentary record formed from a combination of pelagic and current-controlled sedimentation; thus any reworking or erosion of deposits has resulted from bottom-current activity. The depositional system covers an area > 70.000 km^2 and spans a modern water-depth range of ~3400 m to >5000 m (excluding shallower seamounts) (Fig. 1). Thus its sedimentary record has the potential to elucidate the effects of abyssal currents at varying depths through time.

In this paper we examine the Cretaceous through present evolution of North Atlantic deep-water circulation, with a focus on the Middle Eocene and younger sedimentary sequence, as delineated by seismic-stratigraphic analysis of contourite drifts on the Newfoundland ridges. We use high-resolution seismic-reflection data coupled with lithologic, biostratigraphic, magnetostratigraphic, and sediment physical-property data obtained from boreholes during Integrated Ocean Drilling Program (IODP) Exp 342 (Norris et al., 2014). Our analysis focuses on sedimentary packages that have distinct internal architecture and mappable boundaries that are tied to age control from IODP Exp 342 cores, which allows us to interpret the history of deep-ocean circulation and compare it to climate history.

2. Geologic background

2.1. Geologic evolution of the J-Anomaly Ridge and Southeast Newfoundland Ridge

Opening of the central North Atlantic Ocean started during the Middle Jurassic, creating a transform boundary along the southwest margin of the Grand Banks offshore Newfoundland (Fig. 1) (Tucholke and Ludwig, 1982; Pe-Piper et al., 2007). Separation of Newfoundland from Iberia began at the end of Jurassic time (e.g., Tucholke et al., 2007) and was followed by rifting that propagated northward, opening the Labrador Sea and finally the northeastern Atlantic Ocean (e.g., Pe-Piper et al., 2007).

The Southeast Newfoundland Ridge (SENR), a positive bathymetric feature extending southeast from the Grand Banks, has been interpreted as a volcanic edifice overlying the intersection of the transform margin and the axis of the rift between Newfoundland and Iberia (Tucholke and Ludwig, 1982; Tucholke et al., 2007). The J-Anomaly Ridge (JAR) extends southwest from, and perpendicular to the orientation of the SENR; it is a topographic high associated with a high-amplitude magnetic anomaly formed about the time of anomaly M0 (Rabinowitz et al., 1978; Sullivan, 1983; Tucholke et al., 1989). The main body of the SENR presently lies at ~3400 to 5000 m depth, and the JAR is ~4000 to 5000 m deep (Fig. 1).

Several prominent volcanic seamounts on the northern part of the SENR rise 500–1000 m above adjacent seafloor to depths of 2500 m. Seismic-reflection data clearly show layered sediments atop these seamounts, but these sediments are unsampled and their stratigraphy cannot be seismically correlated across the steep flanks of the seamounts to the stratigraphy of the surrounding seafloor.

The basement of the JAR and SENR is interpreted to be oceanic, with the conjoined edifices formed above a mantle plume primarily between chrons M4 to younger than M0 (Barremian to Aptian time) during the opening of the Newfoundland-Iberia rift (Tucholke and Ludwig, 1982; Sullivan, 1983; Tucholke et al., 1979, 2007; Norris et al., 2014). The young age limit of magmatism and the relative timing of effusive volcanism in various parts of the Newfoundland ridges are unknown, but magmatism likely did not persist beyond Early Albian time.

Several lines of evidence suggest that the volcanic basement making up at least parts of the SENR and JAR was emergent during its early history. The basement was penetrated by drilling at Deep Sea Drilling Project (DSDP) Site 384 on the southern JAR (Fig. 1), where highly altered tholeiitic basalt with vesicularity typical of water depths <500 m was recovered at 4230 mbsl (Tucholke et al., 1979). The basement core was interpreted as a paleosol formed by subaerial weathering, and it is capped by rudistid reef material of late Barremian/Early Aptian to Early Albian age. The reef material appears subsequently to have been exposed to meteoric waters before subsiding to its present depth. IODP Exp 342 also recovered Albian coral fragments and carbonate-bank deposits that had been exposed to meteoric-water diagenesis at Site U1407 over a basement high on the SENR (Fig. 1) (Norris et al., 2014).

2.2. Modern oceanographic setting

The modern Deep Western Boundary Current (DWBC) is a deep-water thermohaline-driven contour current that intersects the Newfoundland ridges as it flows south along the western margin of the North Atlantic Ocean basin (Fig. 1) (Richardson et al., 1981; Schmitz and McCartney, 1993). Above ~4500 m depth it is sourced in its upper part largely from cooling, sinking surface waters in the Labrador Sea and in its lower part from waters originating in the Norwegian-Greenland Sea (Clarke et al., 1980). The cold, high-salinity deep waters transported in the modern DWBC are collectively referred to as North Atlantic Deep Water (NADW) (McCartney and Talley, 1984; Fine and Molinari, 1988). NADW accounts for approximately 40% of Earth's deep-water formation and thus it is a significant contributor to thermohaline circulation and global heat transfer (Broecker et al., 1998; Talley, 2013). Deep water that flows from the Norwegian-Greenland Sea across the Greenland-Scotland Ridge accounts for a large component of modern NADW (Hansen and Osterhus, 2000). Below ~4500 m, AABW sourced from the circum-Antarctic current follows the path of the DWBC southward along the continental margin south of the Newfoundland ridges (Fig. 1); it circulates primarily in the western North Atlantic basin although AABW components also reach into the northeastern Atlantic (Clarke et al., 1980; McCave and Tucholke, 1986; Dickson and Brown, 1994).

The mean southerly flow of the modern DWBC is probably only 5–10 cm/s, which is sufficient to transport suspended sediment for significant distances but not enough to erode the seafloor (Gardner et al., in press; Hogg, 1983). West of the JAR and SENR along the continental rise of Nova Scotia, the mean speed of the modern DWBC above ~4000 m is estimated to be ~10 cm/s or less (Tucholke et al., 1985). However, currents measured there at greater depths (down to ~5100 m) are highly variable in speed and direction, with speeds sometimes exceeding 70 cm/s and averaging 30 cm/s over a two-week recording period (Richardson et al., 1981). This variability is caused by interaction of the DWBC with the northeasterly flowing Gulf Stream. Details of this interaction are complex and poorly understood (e.g., Clarke et al., 1980; Fofonoff, 1981), but it is apparent that surface eddy kinetic energy (EKE) associated with the Gulf Stream can propagate to the seafloor (abyssal EKE), interacting with the DWBC to generate intermittent and variable high-velocity currents that strongly modify the seabed (Hollister and McCave, 1984). The Gulf Stream path, and its associated high EKE, extend eastward across the JAR and SENR (e.g., McCave and Tucholke, 1986; Savidge and Bane, 1999). Given the fact that the JAR and SENR lie beneath this zone of high EKE, we should expect that energetic bottom currents probably have affected this area since the time that the Gulf Stream first developed.

3. Data

3.1. Seismic-reflection profiles

Fifty-six high-resolution (10–20 m vertical resolution) 2-D seismic-reflection profiles that cover a ~70,000 km^2 area of the JAR and SENR were acquired during Knorr cruise 179–1 (Fig. 1 and Supplementary Fig. S1) (Norris et al., 2004). These data were acquired using the Lamont-Doherty Earth Observatory (LDEO) high-resolution multichannel seismic (MCS) system, which consisted of a 75/75 cubic inch generator-injector (GI) airgun fired at 10 s interval and a solid-state ITI 48-channel streamer with a total length of 600 m towed at 2 m depth and stabilized with depth-keeping birds. The data were digitized at 1 msec. The airgun was configured in true GI mode and floated at a depth of 4 m, which produced a pulse with a spectral peak extending between 30 Hz and 250 Hz and cresting at 90–100 Hz. Despite strong and variable surface currents, the ship maintained a speed over ground of 4.5–4.9 knots. The tightest grid spacing was over the JAR between 51°W to 52°W and 40°N to 40°30′N and also over the SENR near the seamounts between 48°30′W to 50°W and 41°N to 41°45′N (Fig. 1). Grid spacing was 7–14 km over the JAR and 10–18 km in the seamount area. The seismic profiles have a vertical resolution of approximately 8–10 m in shallow sections and up to ~20 m in deeper intervals, and data quality is generally excellent; however, the southern part of line 46 is substandard due to high sea-state during Hurricane Alex (Norris et al., 2004), and it has been used with discretion.

Seismic-reflection data were processed with the SIOSEIS software package. Processing included nulling of six bad traces, application of a frequency-domain, zero-phase bandpass filter with corner frequencies of 35 Hz and 300 Hz, a rolloff of 48 db/octave, and an outside mute. Stacking after normal moveout correction used a single-layer velocity profile based on rms velocity analyses from an earlier Newfoundland

Basin MCS cruise that used a 3.1 km long streamer (Tucholke et al., 1989). The stacked traces were processed with Stolt migration using the velocity of water (1500 m/s) and assuming that the traces were uniformly spaced. Trace amplitude was adjusted using time-varying gain. The seismic-reflection data are publically available and were downloaded from the IODP Site Survey Data Bank (SSDB) for use in this study (Norris et al., 2004).

3.2. Sediment cores

The primary objective of IODP Exp 342 was to acquire contourite drift sediments (Norris et al., 2014), which can provide relatively high-resolution (>3 cm/kyr) archives of climatic and oceanographic change compared to typical pelagic successions (Keigwin and Jones, 1989). Twenty-five holes were cored at nine drill sites (Sites U1403 – U1411; Fig. 1) with a total sediment recovery of ~5400 m. Drill sites were selected using the seismic-reflection data described above to target Paleogene sediments and were drilled along depth transects in order to examine stratification of seawater and changes in ocean chemistry through the Paleogene. Four drill sites targeted drifts on the JAR and the remaining five were drilled in SENR drift accumulations (Fig. 1) (Norris et al., 2014).

Detailed core descriptions were made by the shipboard scientific party and cores were dated using calcareous nannofossils, radiolarians, and foraminifera combined with magnetostratigraphic analysis. Downhole logs were not acquired at any of the drill sites (Norris et al., 2014) so shipboard measurements of core physical properties were used to link core depths to reflection times in seismic-reflection records (see Section 4.3 below). P-wave velocities of cored sediments were obtained using a P-wave Caliper (PWC) tool (Norris et al., 2014) which measures velocities parallel to bedding. We used PWC rather than whole-round (PWL) P-wave measurements; PWC measurements on section halves are higher quality because of better coupling between sensors and the sediment (Norris et al., 2014). Salt-corrected density data were derived using a standard balance to obtain values for dry mass and helium pycnometry to measure volume (Blum, 1997). PWC velocity and density were sampled in 0.5 m increments along the recovered cores.

4. Methods

4.1. Seismic stratigraphic mapping

Vertical and horizontal changes in seismic-reflection facies primarily represent lithologic variations in the sedimentary record, and reflection configurations help to identify processes responsible for sediment transport and deposition as well as sediment availability. Differences in amplitude, concordance, continuity, and geometry of reflections enable the identification and classification of distinct seismic facies (e.g., Sangree and Widmier, 1977; Nielsen et al., 2008; Müller-Michaelis et al., 2013).

We mapped seismic-stratigraphic units, hereafter referred to as seismic units, which are constrained by distinct horizons (H1 to H5) that can be traced throughout the study area. The horizons were defined based on four criteria: (1) onlap, (2) downlap, (3) apparent truncation, and (4) vertical seismic facies change (Fig. 2). Some horizons were not cored and therefore cannot be precisely dated, and some horizons effectively merge where their stratigraphic separation is at or below the vertical resolution of the seismic data (~10–20 m). Because layered sediments on the tops of seamounts cannot be seismically correlated to the stratigraphy of surrounding regions, we excluded these sediments from our interpretation. Schlumberger's seismic-reflection data visualization and interpretation software Petrel® was used to map horizons.

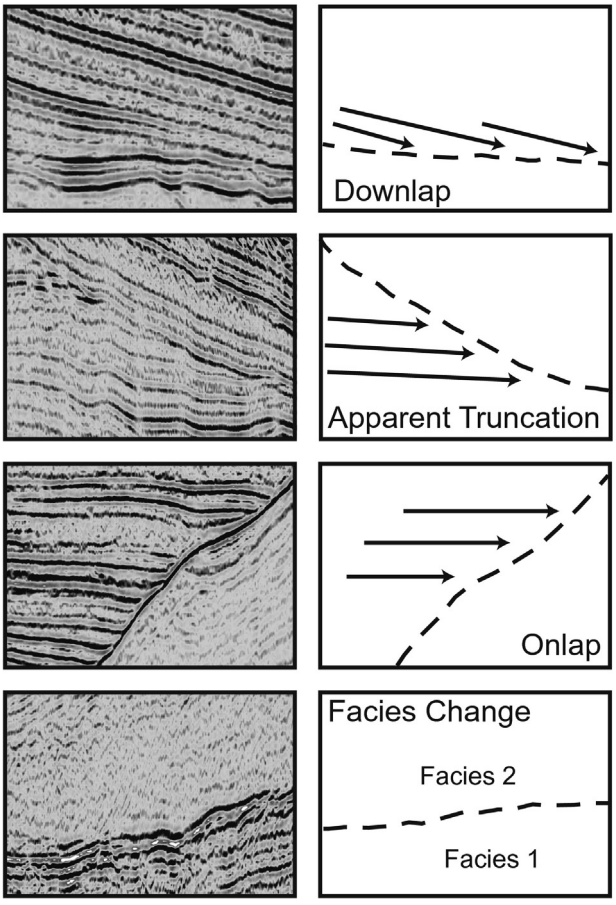

Fig. 2. Criteria used for the identification and mapping of seismic horizons: downlap, truncation, onlap, and abrupt vertical changes in seismic facies.

4.2. Isochron map generation

Stratigraphic thicknesses between horizons were calculated in Petrel® using the 'surface attributes' process and were subsequently used to create isochron maps of each seismic unit. This process calculates thickness in two-way traveltime (TWT) between specified seismic horizons at Common Depth Points (CDP) and assigns the calculated thickness attribute to the stratigraphically younger horizon. Computer-generated isochron maps were produced with a convergent interpolation algorithm, which were biased toward trackline locations. To minimize this limitation, thickness between horizons was converted to point data along tracks, filtered to every 500th CDP (~6 km), and labeled and displayed as a grid of points with thickness values. The computer-generated isochron maps were then overlaid with the point-grid data and final isochron maps were hand contoured.

4.3. Borehole-seismic data correlation

Estimates of seismic horizon depths were obtained by applying average lab-measured PWC velocities to observed reflection-time depths of horizons at the boreholes, progressing from the top to the bottom of the section. Laboratory PWC velocities were measured parallel to bedding, and bedding-parallel velocities are often higher than vertical-incidence velocities because of factors such as grain alignment and preferential cementation of layers (e.g., Tucholke et al., 1976). However, there is probably little such anisotropy in the relatively uniform, seismically transparent drift deposits of Seismic Units 3 and 4. In any case, we consider the PWC velocities to be maximum laboratory values. The laboratory PWC velocities were corrected to in situ pressure and

temperature conditions using the method of Hamilton (1970) with relevant data taken from tables for the speed of sound in seawater (U.S. Naval Oceanographic Office, 1962), bottom-water temperatures from Fuglister (1960), and assuming a geothermal gradient of 0.06 °C m^{-1} in the sediments and a constant pore water salinity of 35‰. The resulting seismic-borehole correlations are summarized in Supplementary Table A and shown graphically in Supplementary Figs. S2–S9.

We also used laboratory density and velocity measurements to generate downhole profiles of acoustic impedance (Supplementary Figs. S2–S9) that helped to guide correlations. Pleistocene sediments of Seismic Unit 5 generally have high impedance (Supplementary Figs. S5–S9). Horizon H4, where present within largely seismically transparent sediment, is associated with generally subtle impedance contrasts (Supplementary Figs. S2–S5 and S8). Horizon H3 in some cases correlates with a marked downward increase in impedance (Supplmentary Figs. S2 and S6) but in most cases the correlation is less well defined.

4.4. Horizon age assignments

Interpreted seismic horizons were assigned ages using chronostratigraphic information from IODP Exp 342 cores (Norris et al., 2014) and are reported using numerical ages and stages from the Gradstein and Ogg (2012) geologic time scale. Not all seismic horizons were penetrated at every drill site because IODP Exp 342 specifically targeted Paleogene drift accumulations (Table 1). Ages were assigned to each horizon via a two-step process: (1) horizon age was determined at each drill site via interpolation between subjacent and superjacent biostratigraphic and/or magnetostratigraphic datums in cores (Norris et al., 2014); (2) these site-specific ages were then averaged to provide an integrated age for each horizon over the entire study area. In cases where a seismic horizon falls within a section of core that is barren of biostratigraphic and/or magnetostratigraphic control, the range of bracketed ages is reported but is not used to calculate an average age (Table 2).

4.5. Volumetric and mass sedimentation rate calculations

Borehole-derived (linear) sediment accumulation rates can vary significantly from site to site in sedimentary systems where deposition is laterally highly nonuniform. Therefore we calculated volumetric accumulation rates for the entire study area (and mass accumulation rates based on volumes) to obtain a more accurate representation of sedimentation history. Using velocities from our seismic/borehole correlations to determine sediment thickness, we calculated bulk volume of each seismic unit from isochron maps, then multiplied the volumes by average, shipboard-measured, salt-corrected dry density (Norris et al., 2014) to compute total sediment mass for each unit. We further estimated terrigenous mass by subtracting the average weight % $CaCO_3$ in each seismic unit (Norris et al., 2014), assuming that the non-carbonate fraction approximates the terrigenous fraction. Finally, we calculated terrigenous mass accumulation rates normalized to 1) the areal extent of each corresponding seismic unit and 2) the 70,000 km^2 areal extent of the entire survey area (Table 3). We consider terrigenous rates to be the most representative of drift accumulation because effects of changes in surface-water productivity and the calcite compensation depth (CCD) are removed. Thus we use terrigenous rates in our discussion.

4.6. Seafloor paleodepths

We estimated seafloor paleodepths to the nearest ~500 m at the times of horizons H3, H4, and H5 using the basement age/depth curve determined at DSDP Site 384 on the J-Anomaly Ridge, correcting for loading by sediment overburden that was present at the time of each horizon (Tucholke and Vogt, 1979).

5. Results

5.1. Seismic units

We identified seven seismic facies, including acoustic basement, and mapped the boundaries of the facies as Horizons H1–H5 (Fig. 3). The six sedimentary facies are treated as five seismic stratigraphic units, with two grouped together as Seismic Unit 4. Each of the five seismic units displays distinctive internal seismic-reflection characteristics; the bounding horizons are regionally mappable and are assigned ages based on IODP Exp 342 borehole results (Fig. 4 and Table 3).

5.1.1. Acoustic basement

Acoustic basement is characterized by moderate- to high-amplitude, discontinuous to chaotic seismic reflections, with an upper boundary defined as seismic Horizon H1 (Figs. 3–7). Horizon H1 is relatively smooth in some areas but more commonly is irregular. Basement age at DSDP Site 384 on the JAR is Late Barremian/Early Aptian, and basement age of the entire JAR/SENR complex may range from Barremian to Early Albian based on magnetic anomalies (Tucholke and Vogt, 1979). In the absence of other data, we assume a basement age of 115 ± 3 Ma (upper Aptian) for Horizon H1 (Table 2).

Basement at DSDP Site 384 subsided unusually rapidly (Tucholke and Vogt, 1979), but it is not known whether the northern JAR and SENR basement experienced a similar subsidence history. Given that the seamounts in the northern part of the study area are up to ~1700 m shallower than basement at DSDP Site 384, it is likely that their summits were once subaerially exposed. Indeed, the tops of three of the seamounts are relatively flat-topped, suggesting subaerial erosion. Thus acoustic basement surrounding these features likely contains debris eroded from the seamounts and dates to an age younger than the underlying volcanic rocks.

5.1.2. Seismic Unit 1

Seismic Unit 1 exhibits moderate- to high-amplitude, continuous to semi-continuous reflections that downlap and onlap onto acoustic basement (Horizon H1) in multiple directions (Figs. 4–7). The upper boundary of the unit is a sharp contact identified by moderate- to

Table 1
Water depth and borehole penetration depth to seismic horizons.

IODP Exp 342 site	U1403	U1404	U1406	U1407	U1408	U1409	U1410	U1411
Water Depth (mbsl)	4949	4710	3799	3073	3022	3503	3387	3299
Horizon H5 depth (mbsf)	Not resolved	Not resolved	Not resolved	Not resolved	Not resolved	Not resolved	33	Not resolved
Horizon H4 depth (mbsf)	52	155	143	11	14	19	52	22
Horizon H3 depth (mbsf)	136	Not penetrated	243	75	222	99	223	Not penetrated
Horizon H2 depth (mbsf)	Not penetrated	Not penetrated	Not penetrated	249	Not penetrated	Not penetrated	Not penetrated	Not penetrated
Horizon H1 depth (mbsf)	Not penetrated	Not penetrated	Not penetrated	Not penetrated	Not penetrated	Not penetrated	Not penetrated	Not penetrated

Note: Drill site U1405 did not resolve Horizon H5 and did not penetrate any deeper horizons and is excluded from this table.
Note: mbsl = meters below sea level; mbsf = meters below seafloor.

Table 2
Seismic horizon age.

Seismic Horizon	U1403	U1404	U1406	U1407	U1408	U1409	U1410	U1411	DSDP 384	Average
	Age (Ma)	Age (Ma)	Age (Ma)	Age (Ma)	Age (Ma)	Age (Ma)	Age (Ma)	Age (Ma)	Age (Ma)	Horizon Age* (Ma)
Horizon H5	3 (?) [Late Pliocene]	3 (?) [Late Pliocene]	3 (?) [Late Pliocene]	3 (?) [Late Pliocene]	3 (?) [Late Pliocene]	3 (?) [Late Pliocene]	3 (?) [Late Pliocene]	3 (?) [Late Pliocene]	3 (?) [Late Pliocene]	3 (?) [Late Pliocene]
Horizon H4	39** [Bartonian]	25 [Chattian]	26 [Chattian]	1–32‡	11–33‡	26 [Chattian]	24 [Chattian]	18–27‡	–	25 [Chattian]
Horizon H3	49 [Ypresian]	Not penetrated	43 [Lutetian]	47 [Lutetian]	47 [Lutetian]	47 [Lutetian]	48 [Ypresian]	Not penetrated	Upper Lower Eocene	47 [Lutetian]
Horizon H2	Not penetrated	Not penetrated	Not penetrated	98 [Cenomanian]	Not penetrated	Not penetrated	Not penetrated	Not penetrated	–	98 [Cenomanian]
Horizon H1	Not penetrated	Not penetrated	Not penetrated	Not penetrated	Not penetrated	Not penetrated	Not penetrated	Not penetrated	~112–118 [Albian-Aptian]	~112–118 [Albian-Aptian]

Note: Site U1405 did not resolve Horizon H5 and did not penetrate any deeper horizons and is excluded from this table.
Note: Shipboard age model, numerical ages, and stages/epochs use GTS2012 (Gradstein and Ogg, 2012) timescale.
? Inferred age based on regional correlation and relationships; see text for further explanation.
‡ Horizon occurs in section of core that lacks biostratigraphic and magnetostratigraphic data; stratigraphically closest age datums shown; site not used in calculating average horizon age.
* Ages calculated by linear interpolation between subjacent and superjacent ages from shipboard age model (Norris et al., 2014).
** Horizon occurs in section of core with only magnetostratigraphic control (no biostratigraphic information); site not used in calculating average horizon age.

high-amplitude reflection Horizon H2, which dips gently toward the southern portion of the study area where it commonly downlaps onto or converges with Horizon H1 (Figs. 5 and 6). In some areas, internal reflections of Seismic Unit 1 are truncated by overlying Horizon H2 (Fig. 5). Horizon H2 was penetrated only at IODP Site U1407 at a depth of 248 m below the seafloor (mbsf) (Table 1) where a thin (<3 cm) chert bed marks the top of alternating beds of light to dark nannofossil chalk with intervals of dark, organic-rich claystone and rare chert (Norris et al., 2014). Horizon H2 may correlate regionally with this lithofacies, but locally it could be associated with a hiatus as suggested by the truncations in the seismic-reflection data (Fig. 5).

Seismic Unit 1 has a maximum thickness of >0.4 s TWT in the shallow part of the survey area close to the seamounts. Elsewhere the unit thins below the resolution of the seismic-reflection data except in local patches, most notably on the deep eastern flank of the JAR (Fig. 9f). Chronologic information dates Horizon H2 to ~98 Ma (Cenomanian) (Table 2), indicating that Seismic Unit 1 spans ~17 Myr above inferred upper Aptian basement. The basement (Horizon H1) was not sampled on IODP Exp 342.

5.1.3. Seismic Unit 2

Seismic Unit 2 exhibits moderate- to high-amplitude semi-continuous to discontinuous reflections (Fig. 3). Its upper boundary is a moderate- to high-amplitude semi-continuous reflection (Horizon H3) that marks an abrupt transition to overlying seismically transparent sediments (Figs. 4–8). In some areas, Horizon H3 truncates internal reflections in Seismic Unit 2 but in most locations it is parallel or subparallel to those reflections (Figs. 4–8). Horizon H3 dips gently toward the south where it converges with Horizon H2 in the same area where Horizon H2 downlaps onto acoustic basement (Figs. 5 and 6). Horizon H3 is associated with chert-rich intervals in IODP Exp 342 cores; however, few individual chert beds, which are typically <10 cm thick, were measured for PWC velocity by the routine 0.5 m sampling interval, so they are not well represented in impedance profiles (Supplementary Figs. S2–S9). Therefore, we used shipboard descriptions of chert-bed occurrence to help guide borehole-seismic ties. Horizon H3 was penetrated at six IODP drill sites (U1403 and U1406–U1410; Figs. 3 and 4). Based on shipboard chronology, the horizon dates to ~47 Ma (Ypresian, or upper lower Eocene) (Table 2), indicating that Seismic Unit 2 was deposited over a period of ~51 Myr.

Cores from Seismic Unit 2 contain nannofossil ooze/chalk and biosiliceous ooze/chalk interbedded with claystone and chert (Fig. 10) (Norris et al., 2014). This lithologic variation causes significant vertical variability in acoustic impedance below Horizon H3 (Supplementary Figs. S2–S9). The unit has a maximum thickness > 0.4 s TWT over the shallower parts of the JAR and SENR and thins to below the resolution of the seismic data in most of the deeper, southern part of the survey area (Fig. 9e).

5.1.4. Seismic Unit 3

Seismic Unit 3 is a seismically transparent interval overall but has low-amplitude reflections in some locations (Fig. 3). Most observable reflections are near the base of the unit where in places they lap onto underlying Horizon H3 (Figs. 4–8). The upper boundary of the unit, Horizon H4 (Fig. 3), is difficult to pinpoint within the seismically transparent drift deposits in some profiles. In some places, the horizon effectively merges with, and is indistinguishable from, the seafloor (Figs. 4b and 5). Horizon H4 was penetrated at three IODP sites on the JAR and five on the SENR, and it shows different seismic expression in the two areas. The JAR drill sites generally show an uphole change to

Table 3
Volumetric and mass accumulation rates.

Seismic unit	Age span (Ma)	Mapped area (km^2)	Bulk Seismic volume (km^3)	Unit duration (Myr)	Bulk vol. accum. rate (km^3/Myr)	Bulk dry density* (kg/m^3)	Sediment mass (Mt)	Mass accum. rate (Mt/kyr)	Non-$CaCO_3$ Fraction**	Non-$CaCO_3$ mass accum. rate‡ (Mt/km^2/Myr)	Non-$CaCO_3$ mass accum. rate^ (Mt/km^2/Myr)
5	3–0	37,229	3939	3	1313	834	3.3E + 06	1095	0.82	24.1	12.8
4	25–3	48,746	26,570	22	1208	760	1.6E + 07	722	0.82	15.4	10.8
3	47–25	60,962	16,375	22	744	1010	1.6E + 07	749	0.66	8.1	7.1
2	98–47	46,661	6441	51	126	1091	6.9E + 06	135	0.30	0.9	0.6
1	115–98	14,452	2018	17	119	1461	2.8E + 06	164	0.30	3.6	0.7

‡ Proxy for terrigneous mass accumulation rate; normalized to mapped area of corresponding seismic unit.
^ Proxy for terrigneous mass accumulation rate; normalized to seismic survey reference area (70,000 km^2); shown graphically in Fig. 11.
* Calculated using shipboard moisture and density (MAD) data from IODP Exp 342 cores (Norris et al., 2014).
** Proxy for terrigenous fraction. Calculated using average non-$CaCO_3$ weight % from shipboard chemistry of IODP Exp 342 cores (Norris et al., 2014).

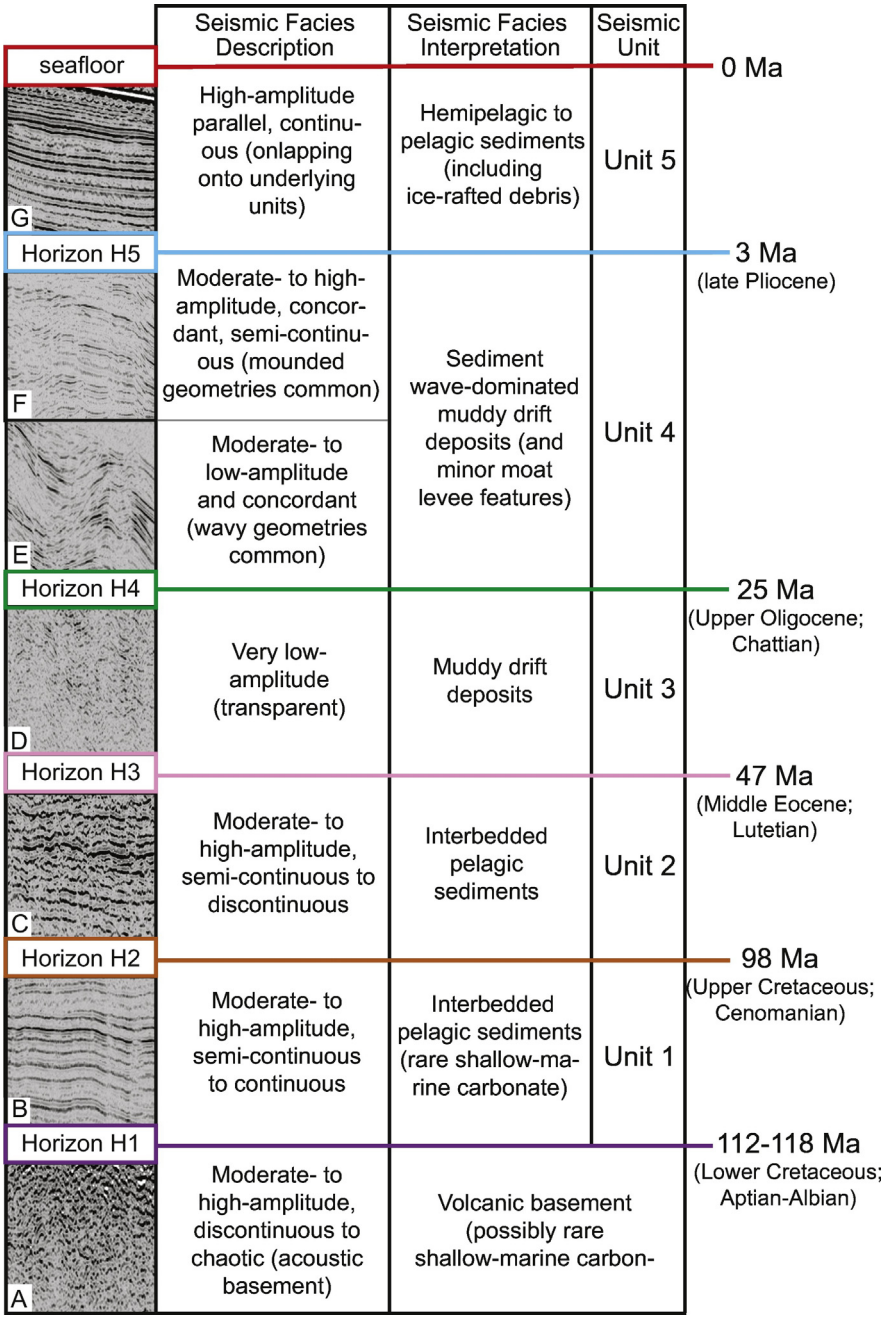

Fig. 3. Seismic Units 1–5, delineated by five horizons (H1–H5) mapped across the survey area. Seismic Units 1, 2, 3, and 5 are characterized by a single, distinct seismic facies (B, C, D, and G, respectively). Seismic Unit 4 consists of two distinct but generally time-equivalent seismic facies (facies E and F) that occur in different areas but are both bounded by underlying Horizon H4 and overlying Horizon H5. Horizon ages are based on seismic-borehole correlations discussed in text and shown in Supplementary Figs. S2–S9. See Table 1 for horizon depths at drill sites and Table 2 for assigned ages.

acoustic impedance values that are lower overall and have reduced variability, but at the five SENR sites, where H4 is associated with a hiatus (or hiatuses) beneath generally much younger and comparatively thin sediments, the uphole change is characterized by increased variability in impedance (Supplementary Figs. S2–S9). Based on chronology from the drill sites, the age of Horizon H4 is ~25 Ma, with the exception of Hole U1403A where the horizon appears to date to ~39 Ma (Table 2). Considering the difficulty of tracing Horizon H4 within the seismically transparent sediments, it is possible that the apparent seismic/borehole correlation at site U1403 (Supplementary Fig. S2) is not valid. For example, if the horizon actually is one cycle (~1 ms) shallower than picked, it would fall at the boundary between Eocene and overlying barren sediments and could well date to a much younger age. For this reason, we discount the 39 Ma age and consider the average age of Horizon H4 to be ~25 Ma (Table 2). Thus Seismic Unit 3 spans a time interval of ~22 Myr.

Sediment cores from Seismic Unit 3 contain thoroughly bioturbated nannofossil clay, clayey nannofossil ooze, and clayey biosiliceous ooze (Fig. 10) (Norris et al., 2014). These sediments have relatively uniform grain size (clay with minor silt) and a homogenous character resulting in diminished acoustic-impedance variability (Supplementary Figs. S2–S9), which is consistent with the mostly transparent seismic expression of the unit (Figs. 3–8). The unit thickness varies significantly across the JAR and SENR. It is thickest in the southern and eastern parts of the

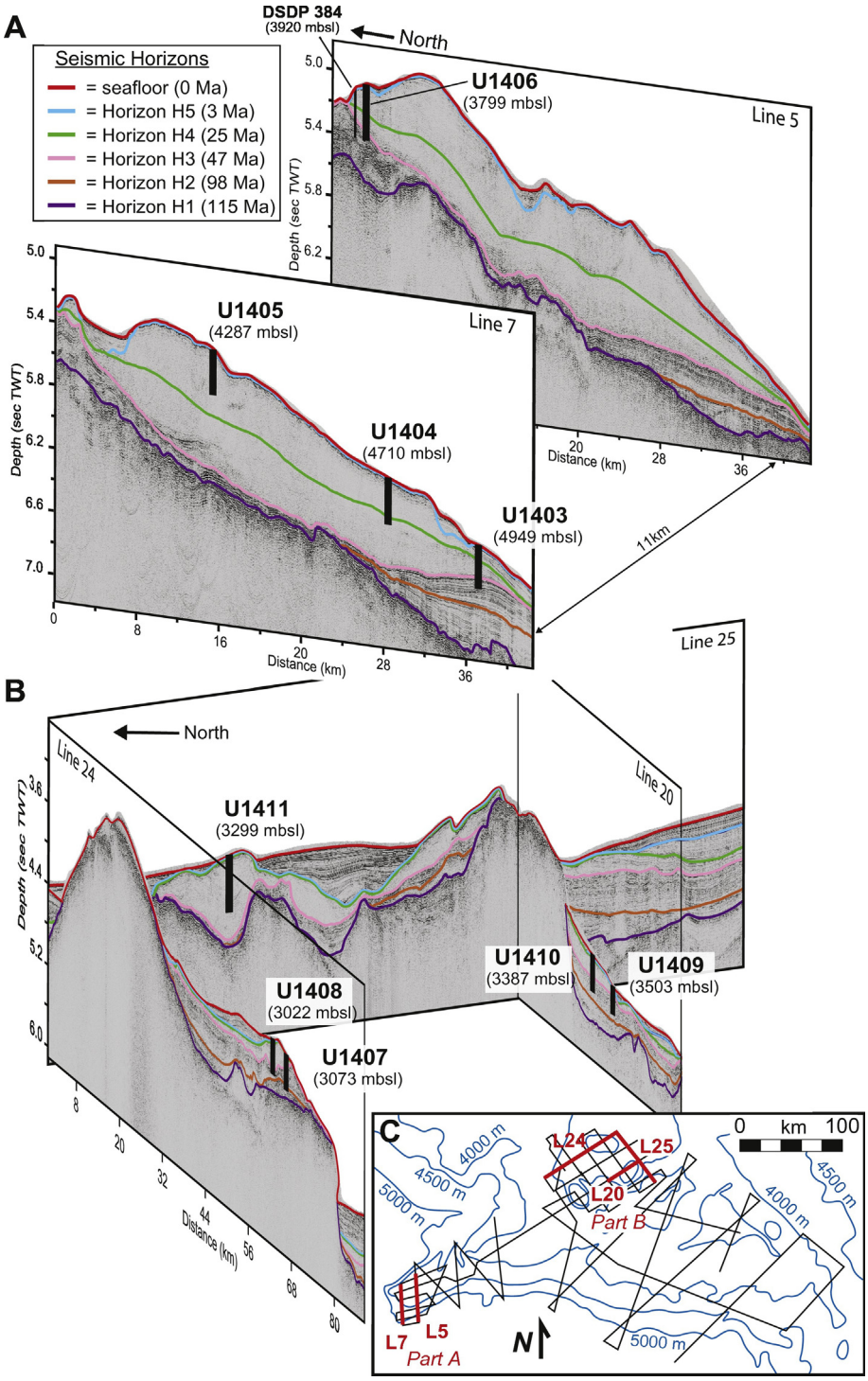

Fig. 4. (a) Perspective image of seismic-reflection profiles along Lines 7 and 5 on the JAR showing the seismic framework and boreholes used to constrain horizon ages. (b) Perspective image of seismic-reflection profiles along Lines 20, 24, and 25 together with boreholes on the SENR. Horizon color explanation in (a) refers to both (a) and (b). (c) Map of study area showing simplified bathymetry and seismic tracklines; illustrated lines are in red. See Fig. 1 for detailed bathymetry and borehole locations. (For interpretation of the references to color in this figure legend, the reader is referred to the web version of this article.)

survey area (locally >1.0 s TWT) and thins below the resolution of the seismic data at the deepest, southern margin of the survey and in patches near the crest of the SENR (Fig. 9d).

5.1.5. Seismic Unit 4

Seismic Unit 4 consists of two distinct seismic facies (Facies E and F; Fig. 3) that occur in different areas but are bounded by underlying Horizon H4 and overlying Horizon H5. Facies E is characterized by low- to moderate-amplitude concordant reflections including prominent wavy internal geometries (Fig. 5). The wavy reflections commonly lap onto underlying Horizon H4 (generally from south to north), are located along the mid to lower margins of the SENR and JAR below ~3500 m water depth, and have variable thickness (up to >1.0 s TWT) (Fig. 9c). The second facies (Facies F) consists of moderate- to high-amplitude, concordant to semi-continuous reflections with a characteristic mounded cross-sectional geometry (Fig. 3). This facies is generally thin (<0.2 s TWT) and mostly restricted to the vicinity of the seamounts on the SENR where it occurs in isolated mounded sediment bodies that downlap

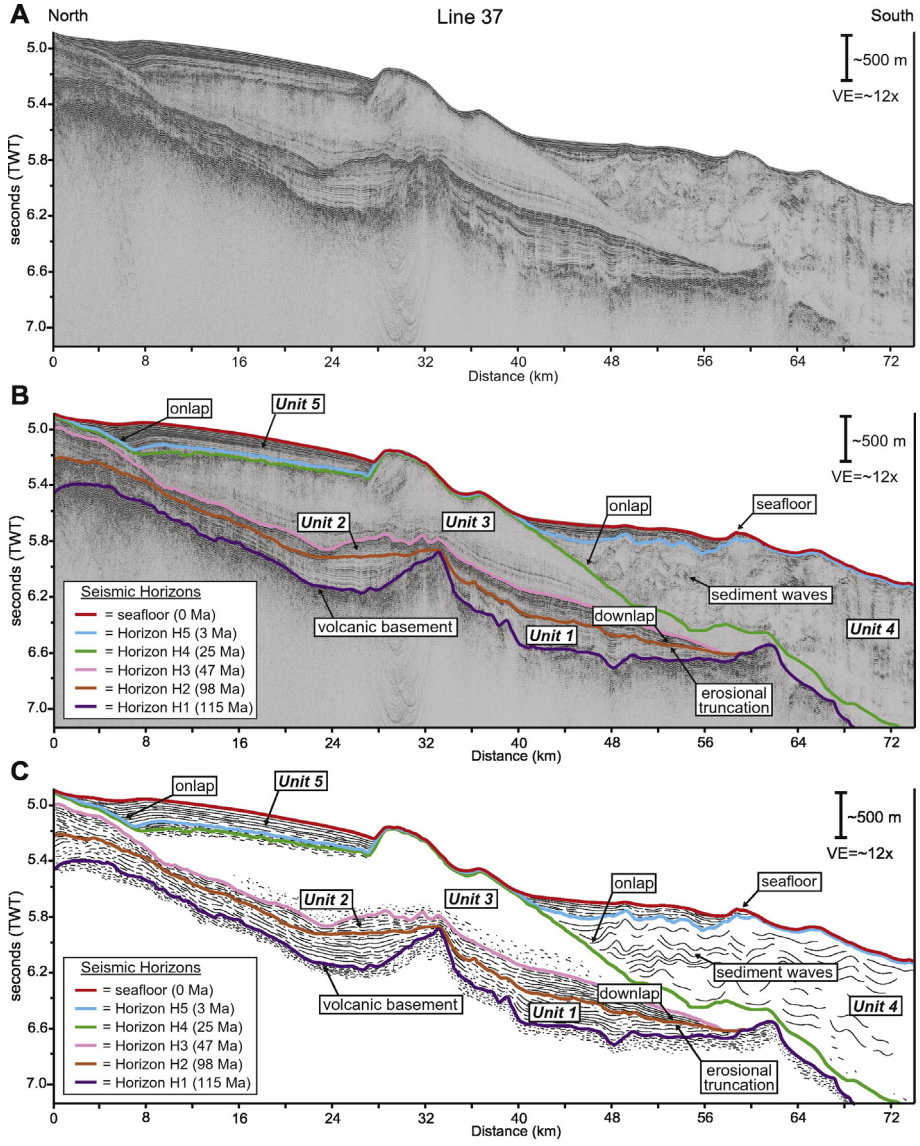

Fig. 5. Seismic-reflection profile Line 37 showing typical seismic-reflection character of the sedimentary sequence on the southern part of the SENR. (a) Uninterpreted profile. (b) Profile with interpreted seismic horizons and seismic units. (c) Line-drawing of interpreted profile. Profile location in Fig. 1.

onto Horizon H4 (Figs. 7 and 9c). Overall, Seismic Unit 4 is thin to absent in the northern part of the SENR where Sites U1407–U1411 are located (Figs. 1 and 9c).

Horizon H5 is variably marked by erosional scours filled with onlapping sediments of overlying Seismic Unit 5 (Fig. 6), by local erosion (Figs. 7, 8), by abrupt vertical facies change to Seismic Unit 5 (Fig. 8), or by merging with the seafloor horizon (Figs. 5 and 6). Horizon H5 is not directly datable with IODP Exp 342 cores because it is within 10–15 m of the seafloor and thus is not separable from the high-amplitude seafloor reflection (Figs. 3–8; Supplementary Figs. S2–S9); the horizon can be identified separately at Site U1410 but there is no age control there. We infer the age of the horizon in two ways. First, there are some similarities between the overlying Seismic Unit 5 and the seismic character and sediment type of stratigraphic intervals documented in other North Atlantic seismic-stratigraphic studies (Arthur et al., 1989; Driscoll and Haug, 1998; Müller-Michaelis et al., 2013; Campbell and Mosher, 2015), and the base of those units is dated at 2.6 Ma. Second, there is strong similarity between the change in seismic character across Horizon 5 and the change at horizons T4 (4 Ma) and Blue (~3 Ma) on the Nova Scotia margin and the U.S. margin farther to the west and southwest, respectively (see Section 6.3). Based on these observations, we assume an age of ~3 Ma for Horizon 5, which would indicate that Seismic Unit 4 spans a time period of ~22 Myr.

Substantial thicknesses of Seismic Unit 4 were cored on the JAR at IODP Sites U1404 through U1406 (Table 1, Fig. 10; Supplementary Figs. S2–S9). The sediment is primarily nannofossil clay and clayey nannofossil ooze (Norris et al., 2014). The general lithologic uniformity of these sediments is apparent in acoustic impedance profiles, particularly that at Site U1404 (Supplementary Fig. S3), which is consistent with the low-amplitude character of the unit in seismic-reflection records (Fig. 6).

5.1.6. Seismic Unit 5

Seismic Unit 5 is composed entirely of moderate- to high-amplitude, parallel and continuous reflections (Figs. 3–8). The upper boundary of this unit is the seafloor and the lower boundary usually is Horizon H5; however, Horizon H4 is the lower boundary in some areas where Seismic Unit 4 is absent (Fig. 7). In either case, reflections at the base of Seismic Unit 5 are variably conformable to non-conformable with underlying deposits, and internal reflections of the unit drape or lap onto the underlying unit (Figs. 3–8). Seismic Unit 5 sediments locally fill depressions (Figs. 6 and 7), which suggests erosion into underlying units,

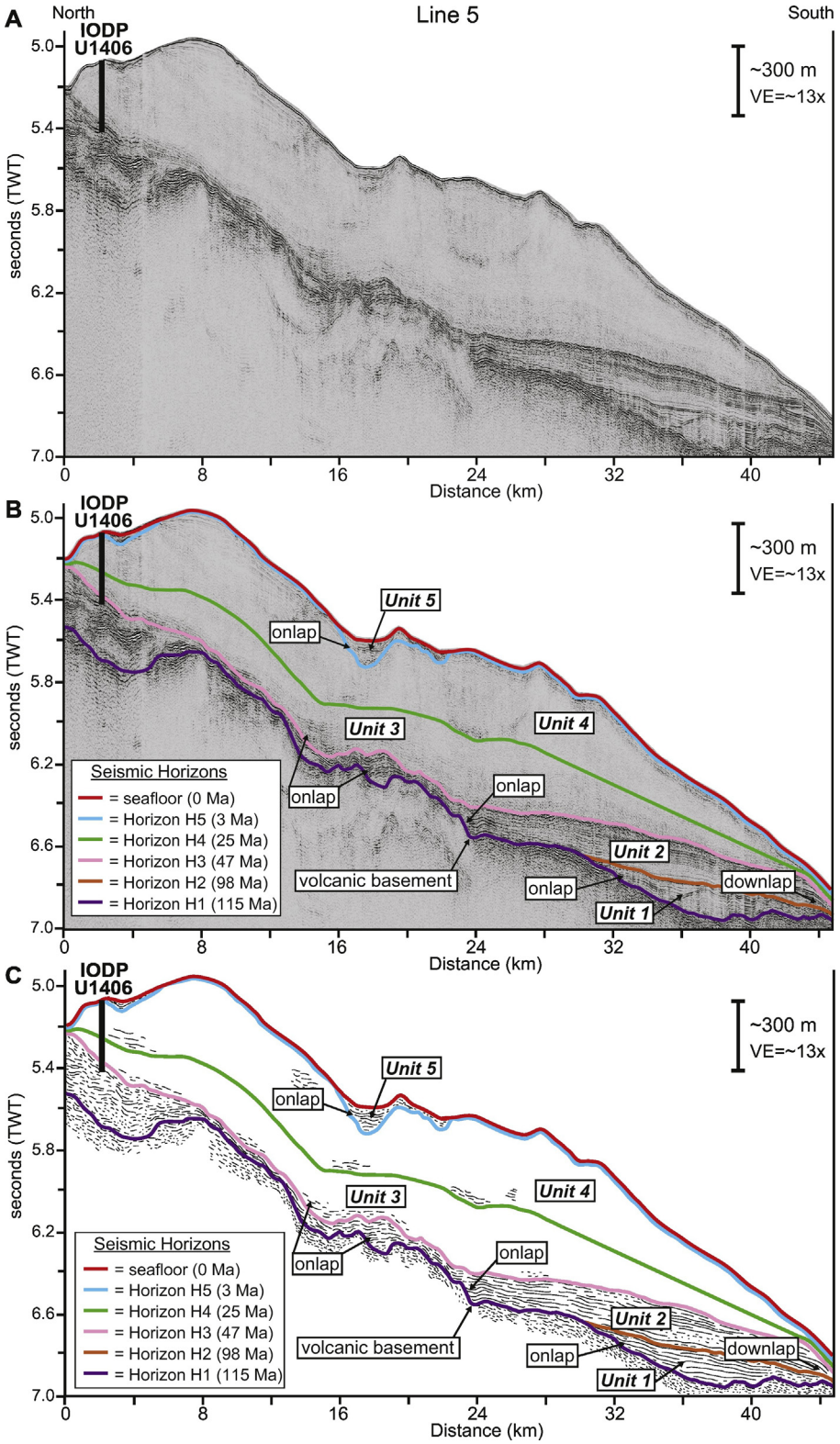

Fig. 6. Seismic-reflection profile Line 5 showing typical seismic-reflection character of the sedimentary sequence on the J-Anomaly Ridge. Location of IODP Exp 342 borehole U1406 is shown. (a) Uninterpreted profile. (b) Profile with interpreted seismic horizons and seismic units. (c) Line-drawing of interpreted profile. Profile location in Fig. 1. See Suppl. Fig. S4 for detailed display at IODP U1406 borehole.

but the lack of clearly truncated reflections in Seismic Unit 4 precludes a definitive interpretation. In other cases, Seismic Unit 5 appears to be filling depressions that are remnant topography related to the wavy and/or mounded features of Seismic Unit 4 (Fig. 5). There are rare occurrences of mounded bodies in Seismic Unit 5 that are similar to those of underlying Seismic Unit 4 in the SENR seamount area, but these are not defining features of the unit.

IODP Exp 342 cores show that Seismic Unit 5 consists primarily of intercalated beds of upper Pliocene and Pleistocene clay, foraminiferal sand, and nannofossil ooze (Fig. 10) (Norris et al., 2014). The cores

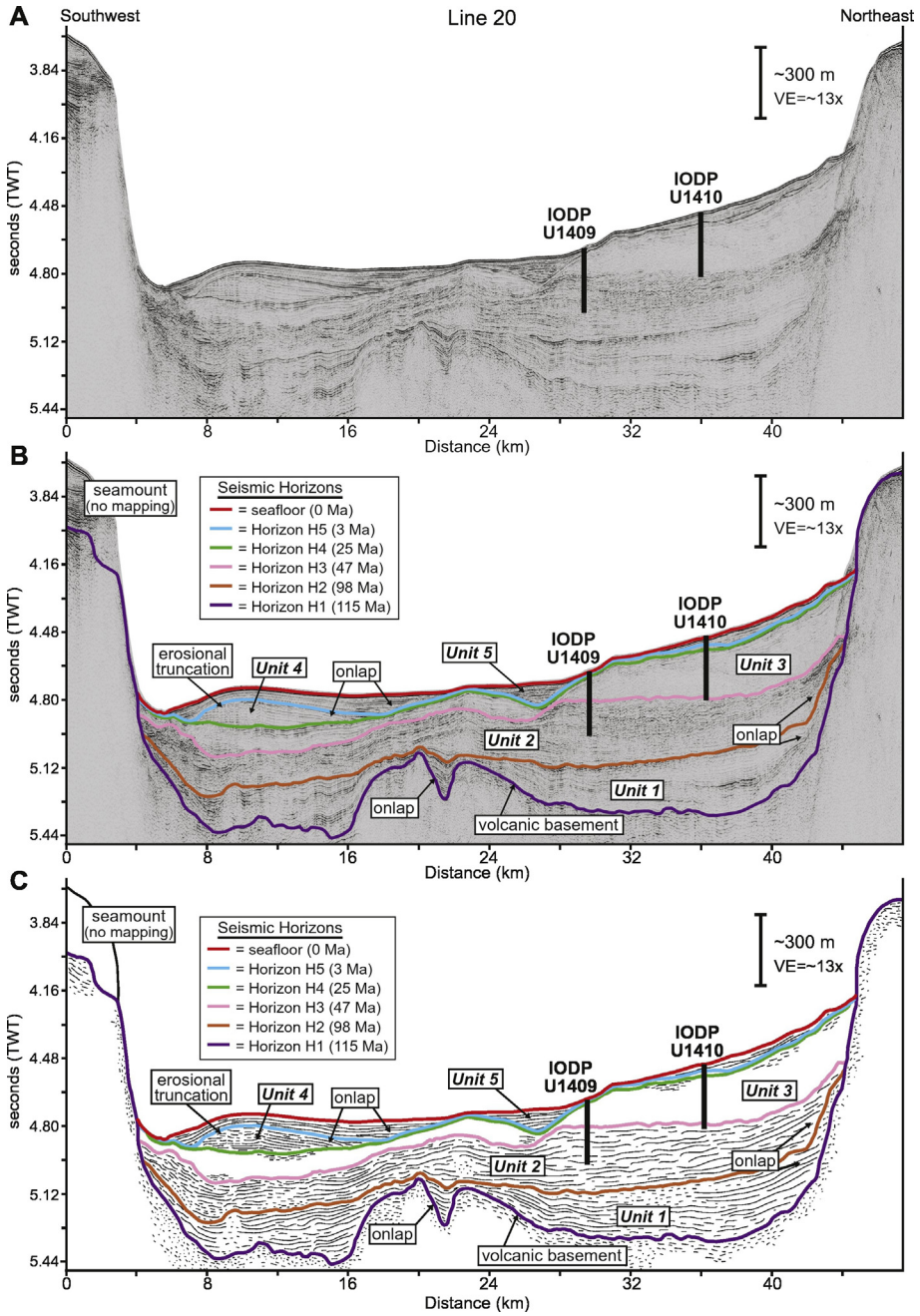

Fig. 7. Seismic-reflection profile Line 20 showing typical seismic-reflection character of the sedimentary sequence on the northern part of the SENR. Locations of IODP Exp 342 boreholes U1409 and U1410 are shown. (a) Uninterpreted profile. (b) Profile with interpreted seismic horizons and seismic units. (c) Line-drawing of interpreted profile. Profile location in Fig. 1. See Suppl. Figs. S7 and S8 for detailed displays at IODP U1409 and U1410 boreholes.

also contain granitic and metamorphic pebbles and cobbles as well as polished quartz and lithic sand grains that are interpreted to be ice-rafted detritus (Norris et al., 2014). The unit is observed only over the shallower parts of the JAR and SENR (up to ~0.4 s TWT in thickness) and in significant turbidite accumulations in much deeper-water areas off the ridges to the south under the Sohm Abyssal Plain (Fig. 9b) and to the north outside the study area. Seismic Unit 5 spans ~3 Myr.

5.2. Sediment accumulation phases

Three primary phases of sedimentation over the SENR and JAR are identified based on our seismic stratigraphic mapping: (1) Pre-Contourite Phase, (2) Active-Contourite Phase, and (3) Late-Contourite Phase (Fig. 11). Seismic Units 1 and 2 represent the Pre-Contourite Phase (~115 Ma to 47 Ma, Late Aptian to the Early-Middle Eocene boundary). Sediments in these units are dominantly calcareous (~70%; Norris et al., 2014) and they had low terrigenous mass accumulation rates compared to overlying units (Table 3). The sediments are not distributed uniformly; the thickest accumulations are mostly in shallower water depths but there are also local thick patches in deeper water (Fig. 9e and f).

The Active-Contourite Phase (47 Ma to 3 Ma; Early-Middle Eocene boundary to ~Late Pliocene) consists of a contourite drift complex recorded in Seismic Units 3 and 4 (Fig. 10). Active-Contourite Phase accumulations form elongate depocenters that generally parallel bathymetric contours and show thicknesses decreasing in up- and down-slope

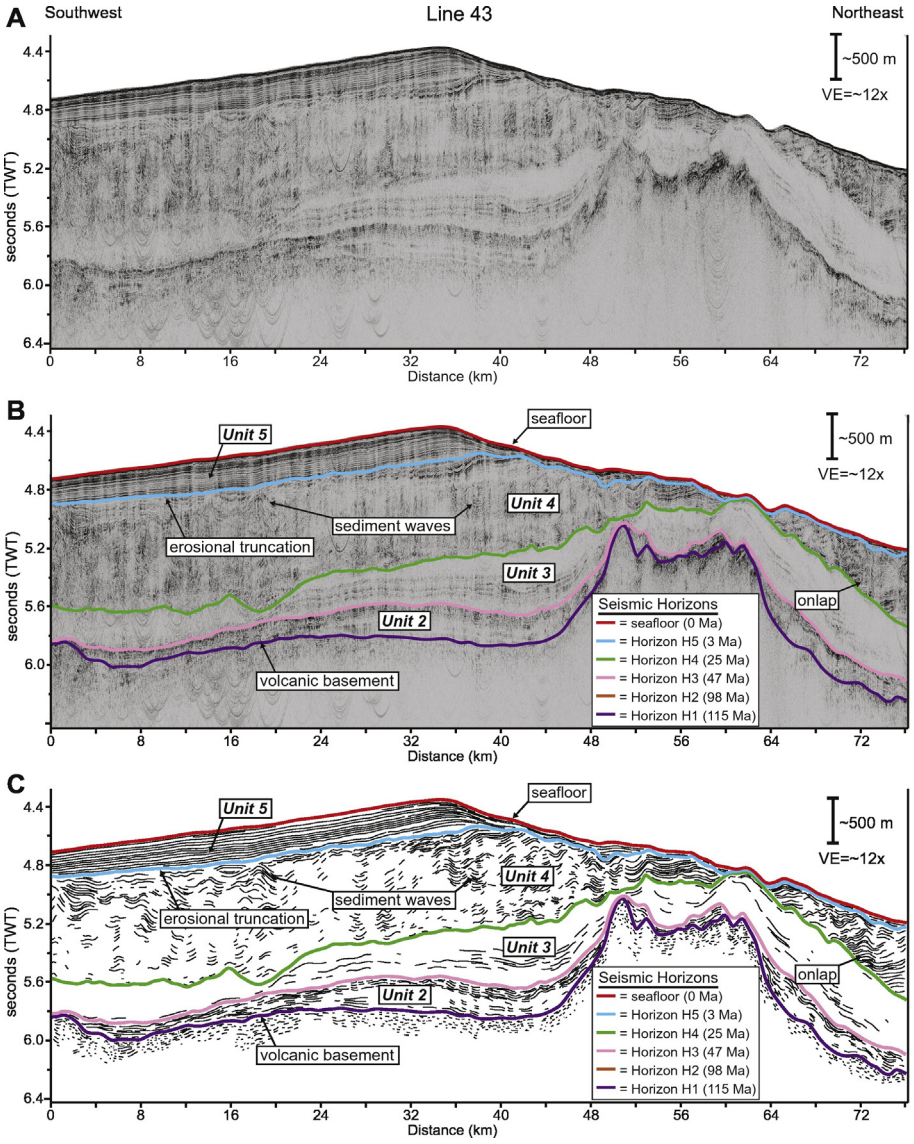

Fig. 8. Seismic-reflection profile Line 43 showing typical seismic-reflection character of the sedimentary sequence on the southeastern part of the SENR. (a) Uninterpreted profile. (b) Profile with interpreted seismic horizons and seismic units. (c) Line-drawing of interpreted profile. Profile location in Fig. 1.

directions (Fig. 9c and d), which are diagnostic features of contourite deposition (McCave and Tucholke, 1986; Faugères et al., 1999; Rebesco and Stow, 2002). Near the SENR seamounts, isolated mounded deposits within Seismic Unit 4 show thickness variations that we interpret to be moat and levee features controlled by local current dynamics around the seamounts. Relative to the Pre-Contourite Phase, sediments deposited during the Active-Contourite Phase are significantly thicker, depocenters shifted toward deeper water (Fig. 9c and d), and a strong terrigenous component appeared (Norris et al., 2014). Terrigenous mass accumulation rates in the Active-Contourite Phase are an order-of-magnitude greater than rates in the Pre-Contourite Phase (Table 3; Fig. 11).

The final phase of deposition (~3 Ma to 0 Ma; Late Pliocene to present) is termed the Late-Contourite Phase and is represented by Seismic Unit 5 (Fig. 11). We designate these deposits as the Late-Contourite Phase due to a change in seismic character associated with the 'modern' deep circulation. Accumulation of Late-Contourite Phase sediment is less spatially extensive than underlying Active-Contourite deposits, with depocenters in the north over shallow seafloor in close proximity to the SENR seamounts (Fig. 9b), but with an increase in terrigenous accumulation rates by a factor of ~1.5 relative to the Active-Contourite Phase (Table 3; Fig. 11).

6. Discussion: North Atlantic Ocean paleo-circulation

6.1. Pre-contourite phase: Cretaceous to Early Eocene pelagic sedimentation

The pattern of Seismic Unit 1 and 2 thicknesses (Fig. 9e and f) suggests two controls on sedimentation. First, the generally thicker accumulations in shallower water are consistent with deposition of the dominantly calcareous sediments above the contemporary CCD (Tucholke and Vogt, 1979). Second, the patchy distribution implies sediment redistribution by currents and/or possibly gravity flows. There is some evidence for local erosion in these units (Fig. 5), and seismic Line 7 across the southern flank of the JAR shows differential deposition that appears to be current controlled (Figs. 4 and 6). A possible explanation is that sedimentation patterns were affected by currents in an anticyclonic gyre north of the circum-equatorial current that is thought to have existed at the time (Tucholke and McCoy, 1986).

A number of prominent seismic horizons of Cretaceous to Early Eocene age have been mapped elsewhere in the western North Atlantic basin but these are not identified at the Newfoundland ridges. The Maastrichtian Horizon A* seismic reflection found near the U.S.

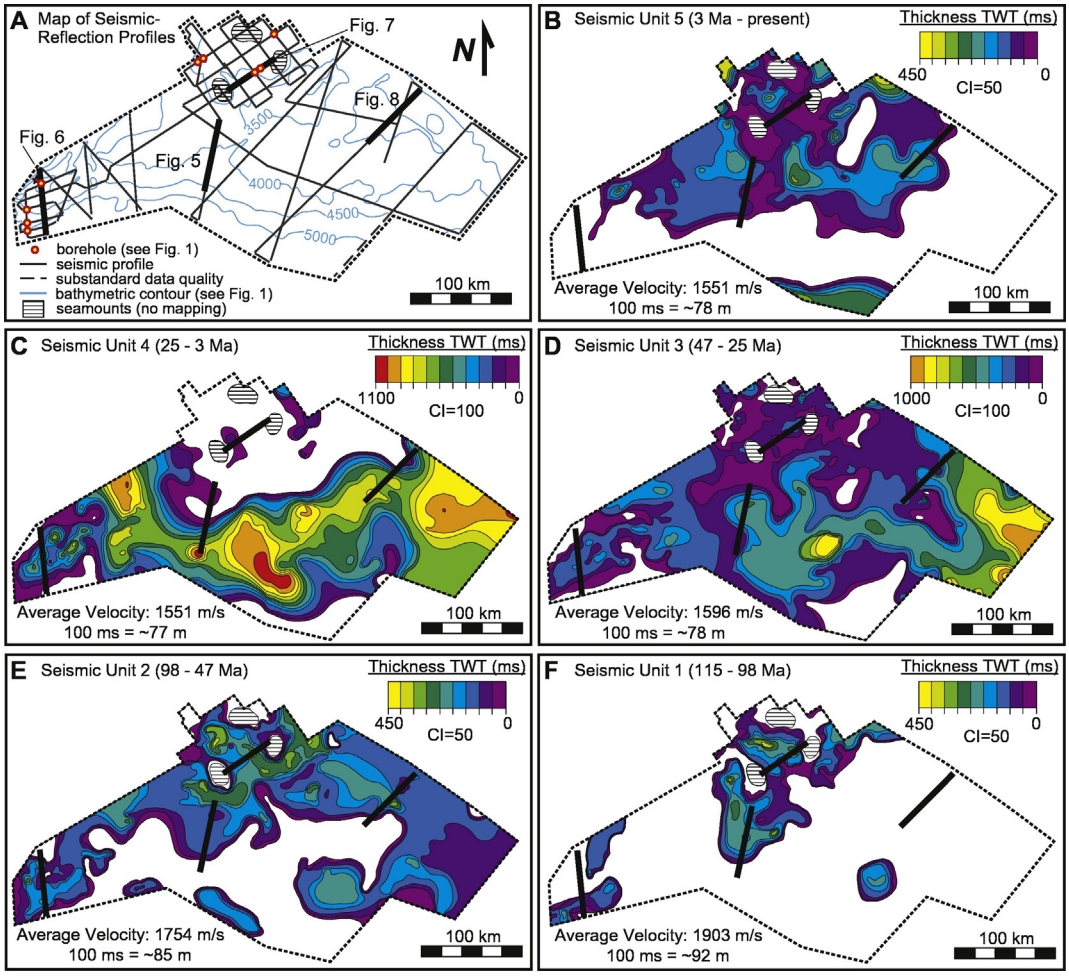

Fig. 9. (a) Track lines of seismic profiles used to map sedimentary sequences. Isochron (thickness) maps of seismic units are displayed in two-way traveltime (TWT, in milliseconds [ms]) for: (b) Seismic Unit 5 (~3 Ma to present); (c) Seismic Unit 4 (~25 to ~3 Ma); (d) Seismic Unit 3 (~47 to ~25 Ma); (e) Seismic Unit 2 (~98 to ~47 Ma); and (f) Seismic Unit 1 (~115 to ~98 Ma). Note isochron scale changes in different panels. Heavy black lines show locations of profiles in Figs. 5–8 (see part a). Refer to Fig. 1 for bathymetry and site numbers of boreholes, to Suppl. Fig. 1 for a map of profile numbers, and to Supplementary Fig. S10 for seismic unit thickness in relation to basement depth.

continental margin and under the western Bermuda Rise (Tucholke, 1979; Mountain and Tucholke, 1985) would be within our Seismic Unit 2 but is not identified there. Horizon A* is the top of a carbonate interval within pelagic clays in the deep North Atlantic basin and is interpreted by Tucholke and Vogt (1979) to be caused by a temporary depression of the CCD. This event of carbonate deposition would not create a prominent, mappable reflection on the JAR/SENR because the Cretaceous to Middle Eocene section there is dominantly carbonates.

In younger sediments of the western North Atlantic basin, Mountain and Miller (1992) mapped a seismic unconformity, termed Horizon A^b, in the Paleocene section on the southern Bermuda Rise, which they interpreted to be the result of erosion by bottom currents sourced from the south ('proto-AABW'). At the time of that event, the southern Bermuda Rise was at depths >5000 m (Tucholke and Vogt, 1979), well below the paleodepth (~3–4 km) of the bulk of the JAR/SENR. Although the currents could have affected sedimentation along the base of the Newfoundland ridges, contemporary sediments there are largely absent (Fig. 9e), so it is difficult to evaluate this possibility. A much shallower (<~2200 m) system of southward-flowing currents was proposed to explain a time-equivalent unconformity on the Blake Nose, offshore Georgia, at the time of the Paleocene-Eocene Thermal Maximum (PETM) (Norris et al., 2001). We did not identify a correlative, regionally mappable horizon associated with unconformity development within Seismic Unit 2 on the shallower parts of the Newfoundland ridges. At the deep Site U1403 on the JAR there is an upward and permanent change from carbonate-free to carbonate-bearing claystones associated with the PETM (Norris et al., 2014; Penman et al., 2016), but it does not produce a regionally distinctive seismic reflection.

6.2. Active-contourite phase

The boundary between Seismic Units 2 and 3 (Horizon H3, ~47 Ma) is marked by an abrupt regional change in seismic facies (Figs. 3-8) and patterns of sediment thickness (Fig. 9), as well as an ~order-of-magnitude increase in terrigenous mass accumulation rates (Table 3; Fig. 11). Above this, Horizon H4 (~25 Ma) is an intra-drift horizon that marks an upward change to more strongly defined depocenters (Fig. 9c). The dominant seismic facies also changed from mostly seismically transparent below H4 to wavy or mounded sequences above on the SENR (Figs. 3, 5, 7, 8) but it remained the same on the JAR (Figs. 4 and 6). Below, we discuss potential correlations of these horizons to other regionally mappable seismic horizons as well as the paleoceanographic implications, with emphasis on the onset of contourite deposition at ~47 Ma, possible changes in sedimentation associated with the Eocene-Oligocene transition, the intra-drift Horizon H4 at ~25 Ma, and the shift to 'modern' deep circulation at ~3 Ma.

6.2.1. Onset of contourite deposition near the Early-Middle Eocene boundary

The transition from Pre-Contourite to Active-Contourite Phase sedimentation is marked by Horizon H3 at ~47 Ma, or earliest Lutetian (just above the Early Eocene-Middle Eocene boundary) (Fig. 11).

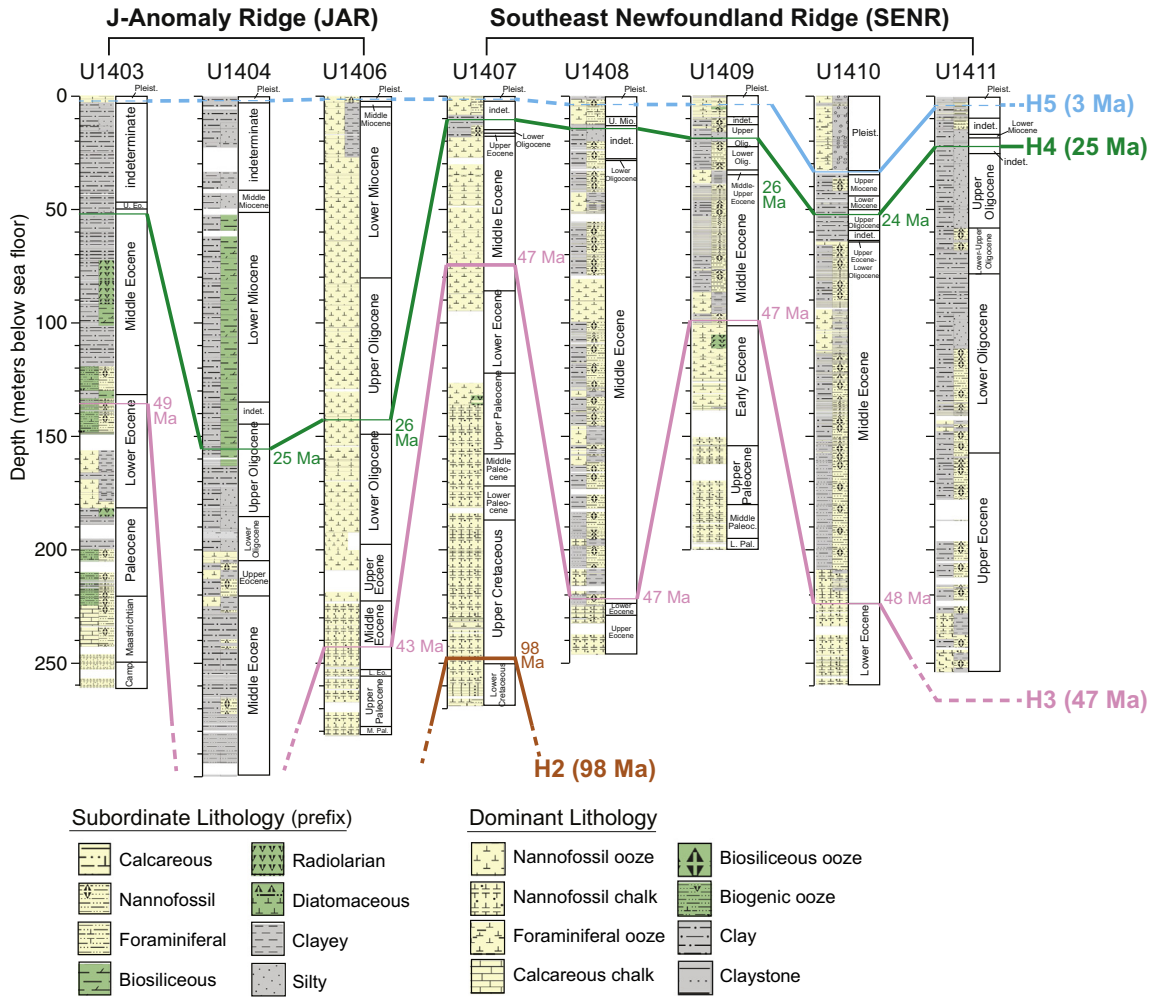

Fig. 10. Correlation chart of IODP Exp 342 drill sites used to constrain seismic stratigraphic framework. See Table 1 for horizon depths, Table 2 for site-specific horizon ages, and Supplementary Figs. S1–S9 for comparison of lithology, physical properties, and seismic-reflection profiles at each site. Lithologic descriptions are from Norris et al. (2014). Site U1405 did not penetrate Horizon H4 or deeper, was not used to constrain horizon ages, and is not shown.

Above this level, Seismic Unit 3 is developed as a 'plastered drift' (McCave and Tucholke, 1986; Faugères et al., 1999). The transition from Seismic Unit 2 to 3 is marked by a five-fold increase in total mass accumulation rate, due mostly to an increase of more than an order-of-magnitude in the terrigenous component (Fig. 11, Table 3). This is consistent with a change in sedimentary regime wherein a newly developed deep current system was able to transport sediments from sources along the northeast Canadian continental margin southward to the topographically isolated Newfoundland ridges.

The onset of drift sedimentation matches a lithologic change in IODP Exp 342 cores from chert-rich oozes/chalks to overlying clay-rich sediments (Norris et al., 2014). The upward disappearance of chert is similar to the lithologic change associated with the widespread, upper-lower to Lower-Middle Eocene Horizon A^C seismic reflection in the deep western North Atlantic south of the Newfoundland ridges (Jansa et al., 1979; Tucholke and Mountain, 1979; Tucholke, 1981; Mountain and Tucholke, 1985). Unlike the advent of current-controlled deposition recorded on the Newfoundland ridges, however, the deep-basin sedimentary sequence overlying Horizon A^C shows no evidence of abyssal current activity (Tucholke and Mountain, 1979; Mountain and Tucholke, 1985).

The situation is somewhat different in the shallower (<~2200 m) sedimentary sequence on the Blake Nose, where ODP Leg 171B found evidence of widespread erosion in otherwise pelagic sediments dating to ~45–50 Ma, with the duration of the hiatus increasing upslope of ~2200 m paleodepth (Norris et al., 2001). The Blake Nose condensed sequence includes cross-bedded, silicified foraminifer sands as well as clay firm-grounds, suggesting both the activity of traction currents and the development of silicified omission surfaces (Norris et al., 1998); these observations are consistent with strong, upper mid-depth bottom currents. The silicified foraminifer sands on Blake Nose are approximately the same age (~48–49 Ma) as Horizon A^C in the deep North Atlantic.

We interpret Horizon H3 to mark the onset of significant deep-current activity in the North Atlantic Ocean that has persisted without notable interruption to the present. It involved the development of terrigenous clay deposition in drifts at intermediate depths on the Newfoundland ridges, produced a change in chert to non-chert lithofacies over a wide depth range, and was associated with active erosion in some shallower sites, such as the Blake Nose. This event is close to the time proposed by Hohbein et al. (2012) for initiation of North Atlantic deep circulation based on a study of the Judd Falls drift in the Faroe-Shetland Channel in the northeast Atlantic. They identified a prominent seismic horizon at the base of this drift that they termed the Intra-Eocene Unconformity (IEU), and they interpreted this to mark the time (49–48 Ma) at which dense waters that formed in the Norwegian-Greenland Sea began to spill over the Greenland-Scotland Ridge.

The onset of this deep circulation corresponds to the end of the period of highest Cenozoic global temperatures, known as the Early Eocene Climatic Optimum (EECO; ~53–51 Ma) (Greenwood and Wing, 1995; Zachos et al., 2001, 2008; Hyland and Sheldon, 2013) and the start of a long-term (~26 Myr) global cooling trend during Middle

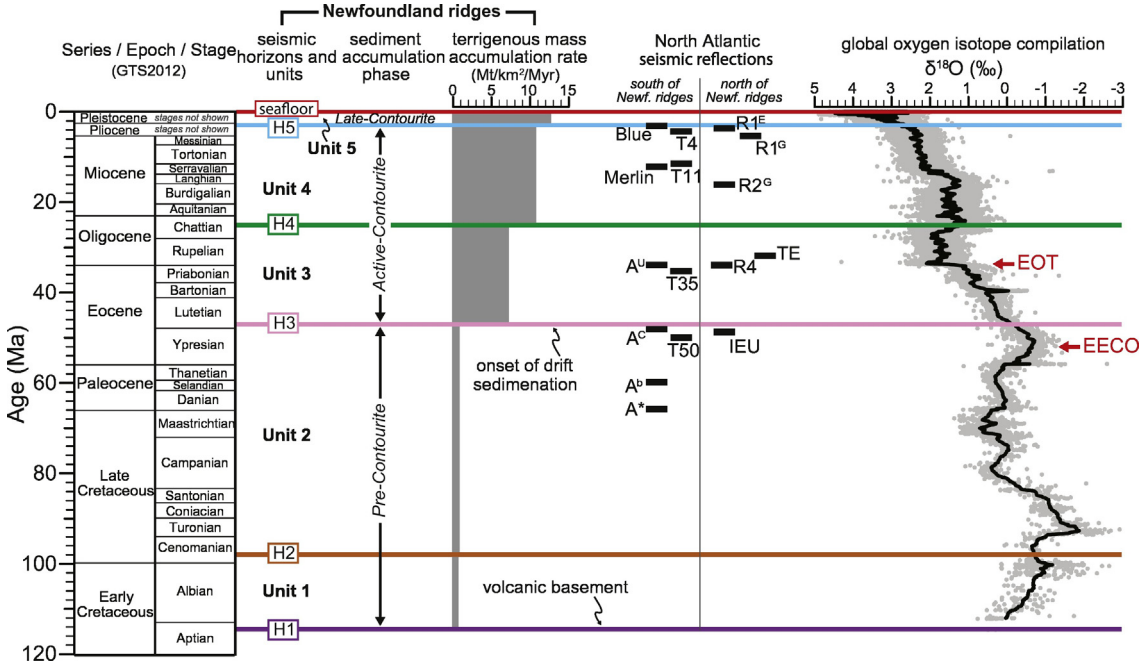

Fig. 11. Chronostratigraphic chart showing seismic horizons, seismic units, sediment accumulation phases, and terrigenous mass accumulation rates (see Table 3) for the JAR and SENR. Ages of other significant seismic reflections in the North Atlantic basins are shown, together with a global oxygen-isotope compilation. Horizons Blue, Merlin, A^U, A^C, A^b, and A* are in the western North Atlantic (Mountain and Miller, 1992; Mountain and Tucholke, 1985; Norris et al., 2001); T4, T11, T35, and T50 are from the Nova Scotia margin (Campbell and Mosher, 2015); $R1^E$ is from Eirik Drift (Arthur et al., 1989; Müller-Michaelis et al., 2013); $R1^G$, $R2^G$, and R4 are from various drift systems in the North Atlantic (Miller and Tucholke, 1983; Wright and Miller, 1996; Miller et al., 2009); TE is from Southeast Faroes Drift (Davies et al., 2001); and IEU is from Judd Falls Drift (Hohbein et al., 2012). The global oxygen isotope compilation (gray points) includes a moving average (black curve); data from Friedrich et al. (2012) and references therein. EECO = Early Eocene Climatic Optimum; EOT = Eocene-Oligocene Transition. (For interpretation of the references to color in this figure legend, the reader is referred to the web version of this article.)

Eocene up to Late Oligocene time (Fig. 11) (Bohaty and Zachos, 2003; Sexton et al., 2006; Jovane et al., 2007; Anagnostou et al., 2016). Aubry (1995) noted that there are hiatuses of this age in many, but not all, regions of the Atlantic Ocean, and Norris et al. (2001) suggested that Horizon A^C (time equivalent to H3 at the Newfoundland ridges) might reflect a global change to more vigorous ocean circulation. It is clear that the start of the Middle Eocene involved changes in ocean chemistry, possibly related to re-organization in ocean overturning, because biosiliceous sedimentation (and subsequent chert formation) largely halted in the North Atlantic at this time (Tucholke and Mountain, 1979; Mountain and Tucholke, 1985).

At the time Seismic Unit 3 was deposited on the Newfoundland ridges, the main part of the drift extended over paleodepths of ~4000–4500 m. We do not know the depth at which the core of the deep current system was active, nor do we know the speed of the current (and thus its potential for seafloor erosion, sediment transport, or deposition) on Myr time scales. If it had a shallow core, then the drift could have been deposited along the deeper, slower reaches of the current system. At shallow paleodepths (<~3000 m) on the Nova Scotia margin to the west, the Early Eocene (50 Ma) Horizon T50 has been interpreted to correlate temporally with Horizon A^C (Campbell et al., 2015), and it is characterized by carbonate-rich lithologies within downslope-oriented gully and ridge topography and, thus, no evidence for current-controlled sedimentation. Erosion documented at depths less than ~2200 m on the Blake Nose (Norris et al., 2001), contemporary with Horizon A^C, could be part of the same current system, which would suggest that the core of the current was indeed at relatively shallow levels.

Another possibility is that the core of the current had average speeds that were appropriate for transportation and deposition of sediments, as opposed to erosion. In this case, the depth distribution of Seismic Unit 3 indicates that the current system was best developed between about 4000 m and 4500 m. A third possibility is that a high-speed current core was present at depths greater than ~4500 m along the continental margin and that the drift was deposited along the upper, slower margin of the flow. Unfortunately, the Eocene sedimentary record that might be used to test this idea farther to the west and south along the continental margin is largely missing. It was removed in Late Eocene to Early Oligocene time by strong abyssal currents at depths of ~5000 m, resulting in the formation of the widespread Horizon A^U unconformity (Tucholke and Mountain, 1979; Mountain and Tucholke, 1985).

From the available evidence, particularly assuming that sediments on the Blake Nose were eroded by the same current system that deposited the Seismic Unit 3 drift, it's possible that the strongest currents were at depths less than ~2000–2500 m and that the drift was deposited along the deeper perimeter of this flow. If this was the case, it seems unlikely that that there were also high-speed currents at depths >4500 m, which would require a 'dual-core' current system. On the other hand, if the shallow-water (<2200 m) erosion on the Blake Nose was caused by currents unrelated to the deep boundary current (e.g., a 'proto-Gulf Stream'), then the core of the deep current could have been near the base of the JAR/SENR, with the plastered drift of Seismic Unit 3 being deposited along its upper reaches.

6.2.2. Changes in drift sedimentation near the Eocene-Oligocene transition

It is noteworthy that the lower part of the Seismic Unit 3 drift (47–25 Ma) is more seismically laminated than the upper part and is relatively conformable to underlying topography (Figs. 5 and 6). The upper part of the drift is more seismically transparent and it exhibits moderate to strong thickness variations that commonly are independent of the underlying topography (Figs. 4-6). In addition, where the drift has been cored at IODP boreholes (Fig. 10), the Oligocene sedimentary section is commonly thin or missing, in contrast to underlying Eocene sediments, most of which are markedly thicker (Supplementary Figs. S2-S9). It is not possible to map thickness patterns of these age units in the low-reflectivity sediments of Seismic Unit 3. However, the changes in seismic and morphologic expression and the marked

thickness differences of the age units at boreholes suggest a significant change in the deep current system during development of Seismic Unit 3.

The change in current regime appears to have occurred in Late Eocene to Early Oligocene time, i.e., at the same time that Horizon A^U was being eroded by strong abyssal currents in the deep (>5000 m) basin to the south (Fig. 11) (Tucholke and Mountain, 1979; Mountain and Tucholke, 1985). The time at which Horizon A^U developed also corresponds to a period of marked erosion by abyssal currents elsewhere in the North Atlantic (Fig. 11). Sedimentary drifts in the northern and northeast North Atlantic (e.g., Gloria, Gardar, Hatton, Feni, and Rockall drifts) contain the widely distributed unconformity Horizon R4, identified as earliest Oligocene in age. This horizon was interpreted by Miller and Tucholke (1983) to represent the onset of northern-sourced, strongly circulating bottom water. In the Faroe-Shetland Basin, Davies et al. (2001) identified lower Oligocene seismic Horizon TE, which they also associated with the onset of current-controlled deposition. On the Nova Scotia continental slope, west of the Newfoundland ridges, Campbell and Mosher (2015) documented modest erosion by abyssal currents in Early Oligocene time (35 Ma, Horizon T35; Fig. 11), and Ebinger and Tucholke (1988) mapped erosion marked by Horizon A^U at greater depths, below the salt front there on the lower continental rise.

Previous studies have noted the correlation of this shift in circulation dynamics to marked global cooling at the Eocene-Oligocene Transition (EOT; ~33–35 Ma) (Fig. 11). The EOT marked the beginning of Cenozoic icehouse conditions and resulted in the formation of dense bottom waters at high latitudes (Coxall and Pearson, 2007, and references therein). (We note that studies of North Atlantic deep circulation in later times [Plio-Pleistocene] show that currents intensified during relatively warm periods and weakened during cool periods [e.g., Bohm et al., 2014; Henry et al., 2016], which seems to be at odds with our interpretation. However, in the Plio-Pleistocene, deep-water formation during cold periods has been suppressed due to the presence of sea ice [e.g., Raymo et al., 1989], and that condition is unlikely to have occurred during the EOT.) We expect that production of these dense waters would intensify the deep current system around the Newfoundland ridges and, if the current had been at shallow to intermediate levels, shift it to greater depths. Thus, it seems likely that during deposition of the Seismic Unit 3 drift, the core of the current system intensified and became established along the deep flanks of the ridges. This evolution would explain why a change in style of deposition occurred during the development of Seismic Unit 3. The lower part of the unit would have been deposited and reworked near the axis of the flow, thus creating impedance contrasts and seismic lamination, while later deposition of the unit would have been beneath slower currents along the upper reaches of a deeper, more intense flow. The paleo-water depth of the Seismic Unit 3 depocenters was no greater than ~4500 m (at the southeastern limit of the seismic survey; Fig. 9d). Therefore, strong abyssal currents below that depth could have formed the Horizon A^U erosional unconformity along the deep eastern margin of North America while at the same time the upper section of Seismic Unit 3 was being deposited beneath shallower, weaker currents.

6.2.3. Late Oligocene to Pliocene drift deposition

Seismic Unit 4 was deposited between Middle-Late Oligocene and Late Pliocene time (~25 Ma to ~3 Ma; Table 2). On the SENR, Horizon H4 marks a change from the seismically transparent facies of the upper part of Seismic Unit 3 to a wavy or mounded seismic facies in Seismic Unit 4 (Figs. 5, 7, and 8). On the JAR, however, Horizon H4 has a more subtle expression within dominantly transparent seismic facies (Figs. 4a and 6), although it is mappable and can be correlated to the SENR. We did not identify clear truncation of underlying Horizon H3 (~47 Ma) by Horizon H4, but the seismically transparent character of the upper part of Seismic Unit 3 makes it difficult to observe whether such erosion may have occurred. We interpret the wavy seismic facies of Seismic Unit 4 on the deeper parts of the SENR to represent muddy sediment waves. Apparent wavelengths are kilometer-scale with amplitudes of 10′s of meters (Figs. 5, 8), similar in dimensions to deep-current-deposited sediment waves described elsewhere (Faugères et al., 1999, and references therein). Mounded features near the SENR seamounts (Fig. 7) are interpreted to be moat-levee deposits that developed from interaction of bottom currents with the seamounts (e.g., Faugères et al., 1999; Stow et al., 2002).

Like Seismic Unit 3, Seismic Unit 4 is a plastered drift but with much greater regional continuity than the underlying Unit 3. The isopach map of this unit shows contour-elongate drift deposits that pinch out both toward shallow water depths on the SENR and toward the deep basin (Fig. 9c), and internal reflections lap onto Horizon H4 in the up-slope (generally northward) direction on parts of the SENR (Fig. 5). The depocenter of the drifts is at nearly the same paleodepth (~3500–4500 m) as that of underlying Seismic Unit 3 (Fig. 9d). The most striking difference with the underlying seismic unit is the near-absence of Seismic Unit 4 at paleodepths less than ~3500 m. The moderate-amplitude reflection character of the sediment waves and the levee deposits on the SENR also suggest a more 'bedded' stratigraphy (i.e., vertical grain-size variation) compared to the transparent character of underlying Seismic Unit 3 (Figs. 5, 7, and 8). However, IODP sites did not penetrate any of these features and therefore the lithology of the deposits cannot be directly related to the seismic architecture. Intervals of Seismic Unit 4 were recovered on the JAR where the seismic facies is more transparent than the equivalent units on SENR (Fig. 6); those sediments are nannofossil-rich clay and clayey nannofossil ooze (Norris et al., 2014).

The general coincidence in location of Seismic Units 3 and 4 (Fig. 9c,d) suggests that the depth and pathway of the deep circulation did not change significantly after Seismic Unit 3 was deposited. However, Horizon H4 developed at a time when the deep oceans warmed (and/or continental ice volume diminished) near the end of the Oligocene (Fig. 11); this climatic warming could have reduced the supply of dense bottom water to the North Atlantic and thus reduced deep-current intensity. This is consistent with a general reduction of current strength through the Oligocene and Early Miocene that is documented to the west along the Nova Scotia margin (Campbell and Mosher, 2015). Mountain and Tucholke (1985) recognized a similar reduction in abyssal circulation farther south along the U.S. Atlantic margin during this period, with major sediment drifts (Blake, Bahama, Chesapeake and Hatteras) beginning to nucleate by Early Miocene time. At the Newfoundland ridges, reduced current strength may explain the observed pattern of drift deposition in Seismic Unit 4, namely that sediments were transported and deposited along the axis of the flow between about ~3500–4500 m paleodepth, with sediment accumulation being very limited in shallower, more tranquil areas.

On the Nova Scotia margin Campbell and Mosher (2015) documented a brief episode of erosion by bottom currents that occurred during the period when Seismic Unit 4 was being deposited (earliest Late Miocene; horizon T11 at 11 Ma) (Fig. 11). A similar, and most likely coeval, event (horizon Merlin) was identified by Mountain and Tucholke (1985) on the U.S. continental margin, which was interpreted to be Late Middle Miocene age. In both areas, well-developed sediment drifts with migrating sediment waves developed above the unconformity. In the northern North Atlantic, a widespread and essentially coeval unconformity (Late Middle Miocene) has also been documented between horizons R2 and R1 (Miller and Tucholke, 1983). The current pulse that caused this erosion near the end of the Middle Miocene in all these regions occurred at a time when global ocean temperatures were again cooling (Fig. 11), which suggests that denser waters were once again introduced into the deep North Atlantic, presumably strengthening the deep circulation.

No reflection correlating with this brief erosional episode has been identified in Seismic Unit 4 on the Newfoundland ridges, and the distribution of boreholes is not adequate to resolve how drift construction there may have responded to such a change in deep circulation. On

the SENR, Sites U1407-U1411 (Figs. 1, 4b, and 7) targeted Eocene to lower Oligocene sediments in areas where the upper Oligocene-Pliocene section is strongly condensed (Norris et al., 2014). In contrast, Sites U1404-U1406 on the JAR (Figs. 1, 4a, and 6) shows that there was rapid drift construction throughout the Late Oligocene to Early Miocene and very little accretion thereafter (Norris et al., 2014). At the deepest site on the JAR (U1403, ~4950 m), however, this section is very thin (<50 m) or missing (Supplementary Fig. S1), presumably because swift currents were eroding the seafloor or preventing deposition.

By analogy with the post-Merlin/T11 development of sediment waves observed in drifts along the continental margin to the west, we speculate that the parts of Seismic Unit 4 that exhibit sediment waves on the eastern SENR are predominantly of Late Miocene age. If this is correct, there was a significant shift from deposition on the JAR in the Late Oligocene to Early Miocene, to deposition on the eastern SENR in the Late Miocene. As noted previously, the general depth and pathway of the deep circulation probably did not change significantly; instead, changes in current strength would have been responsible for reorganization of the drift depocenters within Seismic Unit 4. Drilling on the eastern SENR is needed to fully understand how drift deposition may have shifted during Late Oligocene to Pliocene time.

6.3. Late-contourite phase: Late Pliocene to quaternary sedimentation

Horizon H5 heralded a significant change in the pattern of sediment accumulation on the Newfoundland ridges (Fig. 9b). Where drilled, the horizon is very close to the seafloor and generally is not seismically resolvable from that interface (Fig. 10) except at Site U1410 (Supplementary Fig. S8). At all drill sites, however, it appears to be coincident with a major unconformity between Pleistocene (or age-indeterminate) sediments above, and upper Miocene or older sediments below (Supplementary Figs. S2–S9).

We attribute the unconformity to current-controlled erosion and non-deposition that began by the end of Pliocene time, coincident with marked global cooling (Fig. 11), and we infer that it dates to ~3 Ma (Table 2) based on correlation to stratigraphic architecture of the continental margin farther to the west. On the Nova Scotia continental rise, Campbell and Mosher (2015) documented a Late Pliocene episode of current erosion (T4, 4 Ma) that affected the continental slope there, and farther south Mountain and Tucholke (1985) mapped a similar unconformity (horizon Blue, ~3 Ma) on the U. S. continental rise (Fig. 11). Mountain and Tucholke (1985) suggested that the unconformity was eroded due to enhanced production of bottom water at high latitudes, and Campbell and Mosher (2015) further suggested that it was related to an increased contribution of Labrador Sea Water to the western boundary current system. We consider this ~Late Pliocene event along the continental margin and on the JAR/SENR to reflect the establishment of modern deep circulation in the North Atlantic.

Above Horizon 5, Seismic Unit 5 shows an almost direct reversal of drift spatial accumulation patterns compared to the underlying unit (Figs. 9b,c). The axis of the main depocenter shoaled to paleodepths of about 3500 m, and drift accumulation ceased on the mid to lower parts of the JAR and SENR (Figs. 5 and 6). We interpret the zone of erosion and non-deposition below ~4000 m to be the location of the core of the DWBC, with sediments accumulating only under the shallower, slower reaches of the flow. The depocenter at the southernmost limit of the survey area (Fig. 9b) consists of turbidites beneath the Sohm Abyssal Plain at depths below ~5300 m.

On the north slope of the SENR, seafloor gradient is greater than on the south slope, and topographically intensified flow there has resulted in marked asymmetry of sedimentation and erosion on the two ridge flanks (Fig. 8). This stratigraphic architecture is remarkably similar to the configuration of the Pliocene-Pleistocene section that encompasses horizon Blue on the Blake Outer Ridge (Fig. 8–27 of Mountain and Tucholke (1985). On the SENR to the west, flow perturbed by the seamounts has created irregular sedimentation patterns as well as local truncation of underlying sediments at the level of Horizon H5 (Fig. 7).

The seismically well-laminated sediments of Seismic Unit 5 on elevated parts of the Newfoundland ridges reflect multiple sedimentary processes and variable sediment grain size and/or composition that were associated with fluctuations in continental glaciation. The unit is a thin veneer (below seismic resolution) at most IODP Exp 342 sites and consists of interbedded clay, foraminiferal sand, nannofossil ooze, and outsized clasts interpreted as ice-rafted debris (Norris et al., 2014). Pleistocene glaciations accompanied by lowered sea levels resulted in episodic dominance of down-slope, terrigenous sedimentation on the continental margin to the west (Campbell and Mosher, 2015; Mountain and Tucholke, 1985) and in deep water adjacent to the Newfoundland ridges (e.g., on the Sohm Abyssal Plain). Seismic Unit 5 on the JAR/SENR likewise probably includes terrigenous sediments that were eroded from the Grand Banks. However, these sediments were deposited predominantly from southward-flowing currents and ice rafting rather than from downslope gravity flows because the JAR/SENR was topographically isolated from the Grand Banks (Fig. 1b).

One further process that has influenced deposition and erosion on the Newfoundland ridges since at least Late Pliocene time is interaction with the Gulf Stream, which is thought to have strengthened significantly in the Late Pliocene as the Central American Seaway closed (Bartoli et al., 2005; Haug and Tiedemann, 1998). The JAR and SENR underlie a zone of high abyssal eddy kinetic energy at the base of this flow (McCave and Tucholke, 1986; Savidge and Bane, 1999). Thus, variable but often strong currents there have probably contributed to moat construction near seamounts, to winnowing and sediment transport that have created seismic lamination, and to the generally irregular distribution of Seismic Unit 5 (Fig. 9b). The effect that an earlier 'proto Gulf Stream' may have had on sedimentation on the JAR/SENR, if any, is unknown.

7. Conclusions

We used an integrated data set of seismic-reflection profiles and IODP core data (lithology, biostratigraphy, and magnetostratigraphy) to document the Cretaceous to present sedimentation history on the J-Anomaly Ridge and Southeast Newfoundland Ridge, offshore Newfoundland, Canada. We focused particularly on Middle Eocene and younger sediment drifts and their relationship to the deep paleocirculation history in the North Atlantic. Our results are summarized as follows:

- Initial deposition (Albian through Early Eocene) was dominated by accumulation of calcareous pelagic sediments. Sediment thickness patterns suggest that deposition was controlled by the depth of the CCD and also by limited current activity, possibly related to gyres associated with circum-global equatorial circulation at that time.
- A marked change in deposition patterns occurred ~47 Ma, near the Early/Middle Eocene boundary, when well defined contourite drifts began to aggrade in paleo-water depths between ~4000 and 4500 m, accompanied by an order-of magnitude increase in terrigenous mass accumulation rates. We interpret this to record the time at which geologically significant, persistent deep circulation was initiated in the North Atlantic. This timing is coincident with a general circulation change implied by cessation of biosiliceous sedimentation and subsequent chert formation throughout the western North Atlantic (marked by seismic Horizon A^C) and with seafloor erosion by deep currents that formed the Intra-Eocene Unconformity (IEU) in the northeastern North Atlantic.
- Drift accretion continued through the Middle Eocene to late Oligocene, but a change in style of drift development (i.e., in seismic-stratigraphic facies, morphology, and thickness patterns) occurred within this sequence. We suggest that this change was the result of

deepening and intensification of abyssal currents in late Eocene to Early Oligocene time. Those strong currents caused widespread erosion below ~4500 m along the eastern margin of North America, marked by seismic Horizon A^U.

- By late Oligocene time (~25 Ma), current strength was reduced, terrigenous mass accumulation rates increased slightly, and drift construction was constrained to a well defined zone generally at paleodepths of ~3500–4500 m. Accretion of these drifts correlates with the widespread onset and continuing construction of major sediment drifts throughout the North Atlantic in ~late Oligocene through Miocene-Pliocene time. On the Southeast Newfoundland Ridge the drifts are dominated by laminated mud waves, while more seismically transparent sediments accumulated on the J-Anomaly Ridge. The difference in drift development on the two ridges could be related to shifts in the deep current circulation in ~Middle/Late Miocene time, coincident with formation of drifts dominated by mud waves farther south along the continental margin, but this concept needs to be tested by drilling.
- A significant change to strongly laminated seismic facies occurred in ~late Pliocene time (~3 Ma). This seismic facies corresponds to mixed pelagic-hemipelagic sediments that contain ice-rafted debris and show evidence of glacial-interglacial fluctuations. The locus of drift accumulation shifted markedly with respect to the underlying drifts, with deposition occurring shallower than 4000 m and erosion or non-deposition present at greater depths. We suggest that this change corresponds to establishment of the 'modern' deep circulation system that has persisted to the present.

Supplementary data to this article can be found online at http://dx.doi.org/10.1016/j.margeo.2016.12.014.

Acknowledgements

Acquisition and initial analysis of the seismic reflection data used in this study were funded by NSF Grant OCE-0221012. We thank P. Buhl and E. Scholtz for operation of the MCS system and P. Henkart and T. Bolmer for assistance in seismic processing. Sediment core data were provided by the Integrated Ocean Drilling Program (IODP). We thank the participating scientists, technical staff, and crew of IODP Expedition 342 for the acquisition and shipboard analysis of cores used in this study. IODP and the Department of Geosciences at Virginia Tech provided partial funding for PRB and BWR. PRB also thanks Kenneth A. Eriksson and Benjamin C. Gill for their feedback and guidance while serving on his master's thesis committee.

References

Anagnostou, E., John, E.H., Edgar, K.M., Foster, G.L., Ridgwell, A., Inglis, G.N., Pancost, R.D., Lunt, D.J., Pearson, P.N., 2016. Changing atmospheric CO_2 concentration was the primary driver of Early Cenozoic climate. Nature 533:1–19. http://dx.doi.org/10.1038/nature17423.

Arthur, M.A., Srivastava, S.P., Kaminski, M., Jarrard, R., Osler, J., 1989. Seismic stratigraphy and history of deep circulation and sediment drift development in Baffin Bay and the Labrador Sea. Proc. Ocean Drill. Program Sci. Res. 105, 957–988.

Aubry, M.P., 1995. From chronology to stratigraphy: interpreting the Lower and Middle Eocene stratigraphic record in the Atlantic Ocean. SEPM Spec. Publ. 54, 213–274.

Bartoli, G., Sarnthein, M., Weinelt, M., Erlenkeuser, H., Garbe-Schonberg, D., Lea, D.W., 2005. Final closure of Panama and the onset of northern hemisphere glaciation. Earth Planet. Sci. Lett. 237:33–44. http://dx.doi.org/10.1016/j.epsl.2005.06.020.

Berggren, W.A., Hollister, C.D., 1974. Paleogeography, paleobiology, and the history of circulation in the Atlantic Ocean. In: Hay, W.W. (Ed.), Studies in Paleo-Oceanography. SEPM Special Publication Vol. 20, pp. 126–186.

Blum, P., 1997. Physical properties handbook: a guide to the shipboard measurement of physical properties of deep-sea cores. ODP Technical Note 26:1–11. http://dx.doi.org/10.2973/odp.tn.26.1997.

Bohaty, S.M., Zachos, J.C., 2003. Significant Southern Ocean warming event in the Late Middle Eocene. Geology 31:1017–1020. http://dx.doi.org/10.1130/G19800.1.

Bohm, E., Lippold, J., Gutjahr, M., Frank, M., Blaser, P., Antz, B., Fohlmeister, J., Frank, N., Andersen, M.B., Deininger, M., 2014. Strong and deep Atlantic meridional overturning circulation during the last glacial cycle. Nature 517:73–76. http://dx.doi.org/10.1038/nature14059.

Bower, A.S., Hunt, H.D., 2000. Lagrangian observations of the deep western boundary current in the North Atlantic Ocean. Part I: Large-Scale Pathways and Spreading Rates. J. Phys. Oceanogr. 30:764–783. http://dx.doi.org/10.1175/1520-0485(2000)030<0764:LOOTDW>2.0.CO;2.

Broecker, W.S., Peacock, S.L., Walker, S., Weiss, R., Fahrbach, E., Schroeder, M., Mikolajewicz, U., Heinze, C., Key, R., Peng, T.-H., Rubin, S., 1998. How much deep water is formed in the Southern Ocean? J. Geophys. Res. 103, 15833–15843.

Campbell, D.C., Mosher, D.C., 2015. Geophysical evidence for widespread Cenozoic bottom current activity from the continental margin of Nova Scotia, Canada. Mar. Geol. 378: 237–260. http://dx.doi.org/10.1016/j.margeo.2015.10.005.

Campbell, D.C., Shimeld, J., Deptuck, M.A., Mosher, D.C., 2015. Seismic stratigraphic framework and depositional history of a large Upper Cretaceous and Cenozoic depocenter off southwest Nova Scotia, Canada. Mar. Pet. Geol. 65:22–42. http://dx.doi.org/10.1016/j.marpetgeo.2015.03.016.

Clarke, R.A., Hill, H.W., Reiniger, R.F., Warren, B.A., 1980. Current system south and east of the grand banks of Newfoundland. J. Phys. Oceanogr. http://dx.doi.org/10.1175/1520-0485(1980)010<0025:CSSAEO>2.0.CO;2.

Coxall, H.K., Pearson, P.N., 2007. The Eocene – Oligocene Transition. In: Williams, M., Haywood, A.M., Gregory, F.J., Schmidt, D.N. (Eds.), Deep-Time Perspectives on Climate Change: Marrying Signal from Computer Models and Biological Proxies. The Micropaleontological Society, London, pp. 351–387.

Davies, R.J., Cartwright, J., Pike, J., Line, C., 2001. Early Oligocene initiation of North Atlantic deep water formation. Nature 410:917–920. http://dx.doi.org/10.1038/35073551.

Dickson, R.R., Brown, J., 1994. The production of North Atlantic deep water: sources, rates, and pathways. J. Geophys. Res. 99:12319–12341. http://dx.doi.org/10.1029/94JC00530.

Driscoll, N.W., Haug, G.H., 1998. A short circuit in thermohaline circulation: a cause for northern hemisphere glaciation? Science 282, 436–438.

Ebinger, C.J., Tucholke, B.E., 1988. Marine geology of Sohm Basin, Canadian Atlantic margin. American Association of Petroleum Geologists Bulletin]–>Am. Assoc. Pet. Geol. Bull. 72, 1450–1468.

Faugères, J.C., Stow, D.A.V., Imbert, P., Viana, A., 1999. Seismic features diagnostic of contourite drifts. Mar. Geol. 162:1–38. http://dx.doi.org/10.1016/S0025-3227(99)00068-7.

Fine, R.A., Molinari, R.L., 1988. A continuous deep western boundary current between Abaco (26.5°N) and Barbados (13°N). Deep-Sea Res. 35, 1441–1450.

Fofonoff, N.P., 1981. The Gulf Stream System. In: Warren, B.A., Wunsch, C. (Eds.), Evolution of Physical Oceanography: Scientific Surveys in Honor of Henry Stommel. MIT Press, Cambridge, MA:pp. 112–139 http://dx.doi.org/10.1017/S0022112065241713.

Fuglister, F.C., 1960. Atlantic Ocean Atlas of Temperature and Salinity Profiles and Data from the International Geophysical Year of 1957–1958. Woods Hole Oceanographic Institute, Woods Hole, MA, p. 209.

Gardner, W.D., Tucholke, B.E., Richardson, M.J., Biscaye, P.E., 2017. Benthic storms and nepheloid layers in the western North Atlantic. Mar. Geol. http://dx.doi.org/10.1016/j.margeo.2016.12.012 (in press).

Gradstein, F.M., Ogg, J.G., 2012. The Geologic Timescale 2012. Elsevier, Amsterdam.

Greenwood, D.R., Wing, S.L., 1995. Eocene continental climates and latitudinal temperature gradients. Geology 23:1044–1048. http://dx.doi.org/10.1130/0091-7613(1995)023<1044:ECCALT>2.3.CO;2.

Hamilton, E.L., 1970. Prediction of in-situ acoustic and elastic properties of marine sediments. Geophysics 36, 266–283.

Hansen, B., Osterhus, S., 2000. North Atlantic Nordic Seas exchanges. Prog. Oceanogr. 45: 109–208. http://dx.doi.org/10.1016/S0079-6611(99)00052-X.

Haug, G.H., Tiedemann, R., 1998. Effect of the formation of the Isthmus of Panama on Atlantic Ocean thermohaline circulation. Nature 393:673–676. http://dx.doi.org/10.1038/31447.

Heezen, B.C., Hollister, C., 1964. Deep-Sea current evidence from abyssal sediments. Mar. Geol. 1, 141–174.

Heezen, B.C., Hollister, C., Ruddiman, W., 1966. Shaping of the continental rise by deep geostrophic currents. Science 152, 502–508.

Henry, L.G., McManus, J.F., Curry, W.B., Roberts, N.L., Piotrowski, A.M., Keigwin, L.D., 2016. North Alantic Ocean circulation and abrupt climate change during the last glaciation. Science 353:470–474. http://dx.doi.org/10.1126/science.aaf5529.

Hogg, N.G., 1983. A note on the deep circulation of the western North Atlantic: its nature and causes. Deep Sea Res. Part A, Oceanogr. Res. Pap. 30:945–961. http://dx.doi.org/10.1016/0198-0149(83)90050-X.

Hohbein, M.W., Sexton, P.F., Cartwright, J.A., 2012. Onset of North Atlantic deep water production coincident with inception of the Cenozoic global cooling trend. Geology 40:255–258. http://dx.doi.org/10.1130/G32461.1.

Hollister, C.D., McCave, I.N., 1984. Sedimentation under deep-sea storms. Nature 309, 220–225.

Hyland, E.G., Sheldon, N.D., 2013. Coupled CO_2-climate response during the Early Eocene climatic optimum. Palaeogeogr. Palaeoclimatol. Palaeoecol. 369:125–135. http://dx.doi.org/10.1016/j.palaeo.2012.10.011.

Jansa, L.F., Enos, P., Tucholke, B.E., Gradstein, F.M., Sheridan, R.E., 1979. Mesozoic-Cenozoic sedimentary formations of the North American Basin: Western North Atlantic. In: Talwani, M., Hay, W., Ryan, W.B.F. (Eds.), Deep Drilling in the Atlantic Ocean: Continental Margins and Paleoenvironment, Maurice Ewing Series 3. American Geophysical Union, Washington, D.C., pp. 1–57.

Jovane, L., Florindo, F., Coccioni, R., Dinares-Turell, J., Marsili, A., Monechi, S., Roberts, A.P., Sprovieri, M., 2007. The middle Eocene climatic optimum event in the Contessa Highway section, Umbrian Apennines, Italy. Bull. Geol. Soc. Am. 119:413–427. http://dx.doi.org/10.1130/B25917.1.

Keigwin, L.D., Jones, G.A., 1989. Glacial-Holocene stratigraphy, chronology, and paleoceanographic observations on some North Atlantic sediment drifts. Deep Sea Res. Part A Oceanogr. Res. Pap. 36:845–867. http://dx.doi.org/10.1016/0198-0149(89)90032-0.

McCartney, M.S., Talley, L.D., 1984. Warm-to-cold water conversion in the Northern North Atlantic Ocean. J. Phys. Oceanogr. http://dx.doi.org/10.1175/1520-0485(1984)014<0922:WTCWCI>2.0.CO;2.
McCave, I.N., Tucholke, B.E., 1986. Deep current-controlled sedimentation in the western North Atlantic. In: Vogt, P.R., Tucholke, B.E. (Eds.), The geology of North AmericaThe Western North Atlantic Region Vol. M. Geological Society of America, Boulder, CO, pp. 451–468.
Meinen, C.S., Watts, D.R., 2000. Vertical structure and transport on a transect across the North Atlantic current near 42°N: time series and mean. J. Geophys. Res. 105: 21869. http://dx.doi.org/10.1029/2000JC900097.
Miller, K.G., Tucholke, B.E., 1983. Development of Cenozoic abyssal circulation south of the Greenland-Scotland Ridge. In: Bott, M.H.P., Saxov, S., Talwani, M., Thiede, J. (Eds.), Structure and Development of the Greenland-Scotland Ridge. Plenum, New York, pp. 549–589.
Miller, K.G., Wright, J.D., Katz, M.E., Wade, B.S., Browning, J.V., Cramer, B.S., Rosenthal, Y., 2009. Climate threshold at the Eocene-Oligocene transition: Antarctic ice sheet influence on ocean circulation. In: Koeberl, C., Montanari, A. (Eds.), The Late Eocene Earth - Hothouse, Icehouse, and Impacts. Geol. Soc. Am. Special Paper 452, pp. 169–178.
Mountain, G., Tucholke, B., 1985. Mesozoic and Cenozoic geology of the U.S. Atlantic continental slope and rise. In: Poag, W. (Ed.), Geologic Evolution of the United States Atlantic Margin. Van Nostrand Reinhold, New York, pp. 293–341.
Mountain, G.S., Miller, K.G., 1992. Seismic and geologic evidence for Early Paleogene deepwater circulation in the western North Atlantic. Paleoceanography 7, 423–439.
Müller-Michaelis, A., Uenzelmann-Neben, G., Stein, R., 2013. A revised Early Miocene age for the instigation of the Eirik Drift, offshore southern Greenland: evidence from high-resolution seismic reflection data. Mar. Geol. 340:1–15. http://dx.doi.org/10.1016/j.margeo.2013.04.012.
Nielsen, T., Knutz, P.C., Kuijpers, A., 2008. Seismic expression of contourite depositional systems. Developments in Sedimentology. Elsevier B.V.:pp. 301–321 http://dx.doi.org/10.1016/S0070-4571(08)00216-1.
Norris, R.D., Kroon, D., Klaus, A., et al., 1998. Blake Nose paleoceanographic transect, Western North Atlantic. In: Norris, R.D., Kroon, D., Klaus, A. (Eds.), Proceedings of the Ocean Drilling ProgramInitial Reports 171B. Ocean Drilling Program, College Station, TX, pp. 1–749.
Norris, R.D., Klaus, A., Kroon, D., 2001. Mid-Eocene deep water, the Late Palaeocene thermal maximum and continental slope mass wasting during the cretaceous-Palaeogene impact. Geol. Soc. Lond. Spec. Publ. 183:23–48. http://dx.doi.org/10.1144/GSL.SP.2001.183.01.02.
Norris, R.D., KNR 179-1 Shipboard Party, 2004. Cruise Report: J Anomaly and SE Newfoundland Sediment Drifts, Knorr 179-1. The IODP Site Survey Data Bank. http://ssdb.iodp.org (Access date: September 2012).
Norris, R.D., Wilson, P.A., Blum, P., the Expedition 342 Scientists, 2014. Proceedings IODP, 342. College Station, TX (Integrated Ocean Drilling Program). http://dx.doi.org/10.2204/iodp.proc.342.2014.
U.S. Naval Oceanographic Office, 1962. Tables of Sound Speed in Sea Water. U.S. Naval Oceanographic Office, Washington, D.C.
Pe-Piper, G., Piper, D.J.W., Jansa, L.F., de Jonge, A., 2007. Early Cretaceous opening of the North Atlantic Ocean: implications of the petrology and tectonic setting of the Fogo seamounts off the SW Grand Banks, Newfoundland. Bull. Geol. Soc. Am. 119: 712–724. http://dx.doi.org/10.1130/B26008.1.
Penman, D.E., Kirtland Turner, S., Sexton, P.F., Norris, R.D., Dickson, A.J., Boulila, S., Ridgwell, A., Zeebe, R.E., Zachos, J.C., Cameron, A., Westerhold, T., Rohl, U., 2016. An abyssal carbonate compensation depth overshoot in the aftermath of the Paleocene-Eocene thermal maximum. Nat. Geosci. http://dx.doi.org/10.1038/ngeo2757.
Rabinowitz, P.D., Cande, S.C., Hayes, D.E., Gradstein, F.M., Norman, A.W., Jansa, L.F., 1978. Grand banks and J-anomaly ridge. Science 202, 71–73.
Rahmstorf, S., 2006. Thermohaline Ocean Circulation. In: Elias, S.A. (Ed.), Encyclopedia of Quaternary Sciences. Elsevier, Amsterdam, pp. 1–10.
Raymo, M.E., Ruddimen, W.F., Backman, J., Clement, B.M., Martinson, D.G., 1989. Late Pliocene variation in northern hemisphere ice sheets and North Atlantic deep water circulation. Paleoceanography 4, 413–446.
Rebesco, M., Stow, D., 2002. Seismic expression of contourites and related deposits: a preface. Mar. Geophys. Res. 22:303–308. http://dx.doi.org/10.1023/A:1016316913639.
Rebesco, M., Hernández-Molina, F.J., Van Rooij, D., Wåhlin, A., 2014. Contourites and associated sediments controlled by deep-water circulation processes: state-of-the-art and future considerations. Mar. Geol. 352:111–154. http://dx.doi.org/10.1016/j.margeo.2014.03.011.
Richardson, M.J., Wimbush, M., Mayer, L., 1981. Exceptionally strong near-bottom flows on the continental rise of Nova Scotia. Science 213, 887–888.
Sangree, J.B., Widmier, J.M., 1977. Seismic stratigraphy and global changes of sea level, part 9: seismic interpretation of clastic depositional facies. AAPG Mem. 26, 165–184.
Savidge, D.K., Bane, J.M., 1999. Cyclogenesis in the deep ocean beneath the Gulf stream: 2. Dynamics. J. Geophys. Res. - Oceans Atmos. 104:18127–18140. http://dx.doi.org/10.1029/1999JC900131.
Schmitz, W.J., McCartney, M.S., 1993. On the North Atlantic circulation. Rev. Geophys. 31, 29–49.
Sexton, P.F., Wilson, P.A., Norris, R.D., 2006. Testing the Cenozoic multi-site composite d18O and d13C curves: new mono-specific Eocene records from a single locality, demerara rise (ocean drilling program leg 207). Paleoceanography 21, PA2019. http://dx.doi.org/10.1029/2005PA001253.
Stow, D.A.V., Faugères, J., Howe, J.A., 2002. Bottom currents, contourites and deep-sea sediment drifts: current state-of-the-art. In: Stow, D.A.V., Pudsey, C.J., Howe, J.A., Faugères, J., Viana, A.R. (Eds.), Deep-Water Contourite Systems: Modern Drifts and Ancient Series, Seismic and Sedimentary Characteristics. Geological Society London: pp. 7–20 http://dx.doi.org/10.1144/GSL.MEM.2002.022.01.02.
Sullivan, K.D., 1983. The Newfoundland Basin: ocean-continent boundary and Mesozoic seafloor spreading history. Earth Planet. Sci. Lett. 62:321–339. http://dx.doi.org/10.1016/0012-821X(83)90003-1.
Talley, L.D., 2013. Closure of the global overturning circulation through the Indian, Pacific, and southern oceans: schematics and transports. Oceanography 26:80–97. http://dx.doi.org/10.5670/oceanog.2013.07.
Tucholke, B.E., Ewing, J.I., 1974. Bathymetry and sediment geometry of the Greater Antilles outer ridge and vicinity. Geol. Soc. Am. Bull. 85, 1789–1802.
Tucholke, B.E., Edgar, N.T., Boyce, R.E., 1976. Physical properties of sediments and correlations with acoustic stratigraphy. In: Hollister, C.D., Craddock, C. (Eds.), Initial Reports of the Deep Sea Drilling Project Vol. 35. U.S. Government Printing Office, Washington, D.C., pp. 229–249.
Tucholke, B.E., 1979. Relationships between acoustic stratigraphy and lithostratigraphy in the western North Atlantic Basin. In: Tucholke, B.E., Vogt, P.R. (Eds.), Initial Reports of the Deep Sea Drilling Project Vol. 43. U.S. Government Printing Office, Washington, D.C., pp. 827–846.
Tucholke, B.E., Mountain, G.S., 1979. Seismic stratigraphy, lithostratigraphy and paleosedimentation patterns in the North American Basin. In: Talwani, M., Hay, W., Ryan, W.B.F. (Eds.), Deep Drilling in the Atlantic Ocean: Continental Margins and Paleoenvironment, Maurice Ewing Series 3. American Geophysical Union, Washington, D.C., pp. 58–86.
Tucholke, B.E., Vogt, P.R., 1979. Western North Atlantic: Sedimentary evolution and aspects of tectonic history. In: Tucholke, B.E., Vogt, P.R. (Eds.), Initial Reports of the Deep Sea Drilling Project. U.S. Government Printing Office, Washington, D.C., pp. 791–825.
Tucholke, B.E., Vogt, P.R., Murdmaa, I.O., Rothe, P., Houghton, R.L., Galehouse, J.S., Kaneps, A., McNulty, C.L., Okada, H., Kendrick, J.W., Demars, K.R., McCave, I.N., 1979. Site 384: the Cretaceous/Tertiary boundary, Aptian reefs, and the J-Anomaly Ridge. In: Tucholke, B.E., Vogt, P.R. (Eds.), Initial Reports of the Deep Sea Drilling Project Vol. 43. U.S. Government Printing Office, Washington, D.C.
Tucholke, B.E., 1981. Geological significance of seismic reflectors in the deep western North Atlantic Basin. In: Warme, J.E., Douglas, R.G., Winterer, E.L. (Eds.), The Deep Sea Drilling Project: A Decade of Progress. SEPM Special Publication Vol. 32, pp. 23–37.
Tucholke, B.E., Ludwig, W.J., 1982. Structure and origin of the J Anomaly Ridge, western North Atlantic Ocean. J. Geophys. Res. 87:9389. http://dx.doi.org/10.1029/JB087iB11p09389.
Tucholke, B.E., Hollister, C.D., Biscaye, P.E., Gardner, W.D., 1985. Abyssal current character determined from sediment bedforms on the Nova Scotian continental rise. Mar. Geol. 66, 43–57.
Tucholke, B.E., McCoy, F.W., 1986. Paleogeographic and paleobathymetric evolution of the North Atlantic Ocean. In: Vogt, P.R., Tucholke, B.E. (Eds.), The Geology of North AmericaThe Western North Atlantic Region, Decade of North American Geology Vol. M. Geological Society of America, pp. 589–602.
Tucholke, B.E., Austin Jr., J.A., Uchupi, E., 1989. Crustal Structure and Rift-Drift Evolution of the Newfoundland Basin. In: Tankard, A.J., Balkwill, H.R. (Eds.), Extensional Tectonics and Stratigraphy of the North Atlantic Margins. American Association of Petroleum Geologists Memoir Vol. 36, pp. 247–263.
Tucholke, B.E., Sawyer, D.S., Sibuet, J.-C., 2007. Breakup of the Newfoundland Iberia rift. In: Karner, G.D., Manatschal, G., Pinheiro, L.M. (Eds.), Imaging, Mapping and Modelling Continental Lithosphere Extension and Breakup, Geological Society London, Special Publication. Vol. 282:pp. 9–46. http://dx.doi.org/10.1144/SP282.2.
Wright, J.D., Miller, K.G., 1996. Control of North Atlantic Deep Water circulation by the Greenland-Scotland Ridge. Paleoceanography 11, 157–170.
Zachos, J.C., Pagani, M., Sloan, L., Thomas, E., Billups, K., 2001. Trends, rhythms, and aberrations in global climate 65 Ma to present. Science 80:686–693. http://dx.doi.org/10.1126/science.1059412.
Zachos, J.C., Dickens, G.R., Zeebe, R.E., 2008. An Early Cenozoic perspective on greenhouse warming and carbon-cycle dynamics. Nature 451:279–283. http://dx.doi.org/10.1038/nature06588.